

# **THESIS**

**HERZALLAH LAZHARI**  
**Mechanical engineering**

**Gödöllő**  
**2023**



**Hungarian University of Agriculture and Life Science**  
**Szent István Campus**  
**Mechanical engineering Course**

**ENERGETIC INVESTIGATION OF A COMPRESSOR  
REFRIGERATION CYCLE**

**Primary Supervisor:** Emőd Péter KORZENSZKY, PhD.  
habil. associate professor

**Independent Consultant:** Péter HERMANUCZ, PhD.

**Author:** **HERZALLAH Lazhari**  
TICYFS

**Institute/Department:** Institute of Technology

**Gödöllő**  
**2023**

**INSTITUTE OF TECHNOLOGY MECHANICAL ENGINEERING  
(MSC)**

**Technical development specialization**

**THESIS**

worksheet for

*HERZALLAH Lazhari (TICYFS)*

---

(MSc) student

**Entitled:**

**Energetic investigation of a compressor refrigeration cycle**

---

**Task description:**

This research aims to assess the energy efficiency of a solar-assisted heat pump for sustainable heating. The study investigates system efficiency and energy losses under different conditions, including single vs. dual compressor operation and insulated vs. uninsulated setups. Experiments were conducted at MATE University during July 2023. The hypothesis explores challenges in mitigating losses with dual compressors and expects insulated systems to have lower energy losses. CoolPack software was used to calculate the Coefficient of Performance (COP).

**Department: Mechanical Engineering**

**Consultant:**

**Supervisor:** Dr. Emőd Péter KORZENSZKY Associate Professor, MATE, Institute of Technology

**Submission deadline:** 06 November 2023.

Gödöllő, 01 November 2023.

**Approved**

**Received**

---

(head of department)

---

(host course leader)

---

(student)

As an independent consultant of the author of this thesis I hereby declare that the student took part in the planned consultations.

Gödöllő, 01 November 2023.

*Korzenszky Péter*  

---

(Consultant)

## Table of contents

1. Introduction .....	6
2. Literature review .....	8
2.1. Introduction to the literature review .....	8
2.2. Heat pumps classifications and their applications .....	8
2.2.1. Air source heat pumps .....	8
2.2.2. Water-source heat pumps.....	12
2.2.3. Ground source heat pumps.....	14
2.3. Solar-Assisted Heat Pump.....	17
2.3.1. Technological methods and their applications.....	17
2.3.2. Technological hurdles in SAHP development.....	20
2.4. Heat pumps and refrigeration machines technology .....	21
2.4.1. Definition .....	21
2.4.2. Main components.....	22
2.4.3. Refrigerants.....	25
2.4.4. Refrigeration cycle.....	27
2.5. Energy examination of the system.....	29
2.6. Subcooled and superheated refrigeration cycle.....	33
2.6.1. Subcooling .....	33
2.6.2. Superheating .....	35
2.7. Real cycle .....	35
2.8. Simulation tools for refrigeration systems .....	36
2.8.1. CoolPack .....	36
2.8.2. Coolselector 2 .....	37
2.8.3. Solkane.....	37
3. Materials and methods .....	38
3.1. Materials and equipment .....	38
3.1.1. Flat plate solar collector.....	39
3.1.2. Heat Pump.....	40
3.1.3. Refrigerant .....	41

3.1.4. Storage tank .....	42
3.2. Data collection .....	42
3.2.1. ALMEMO system.....	43
3.2.2. Measuring equipment.....	44
3.3. Control system .....	47
3.4. Description of the experiment .....	47
3.4.1. System insulation strategy .....	47
3.4.2. Adopted calculations.....	49
4. Results and discussion.....	50
4.1. Solar collector integration and ambient conditions affect.....	51
4.1.1. For a single compressor scenario (the first and the third day).....	51
4.1.2. In a dual-compressor scenario (the second and the fourth day).....	53
4.2. Compressor(s) performance analysis .....	56
4.2.1. For a single compressor scenario (the first and the third day).....	56
4.2.2. In a dual-compressor scenario (the second and the fourth day).....	57
4.3. Heat pump efficiency .....	58
4.3.1. Refrigeration cycle analysis .....	59
4.3.2. Analysis of entropy variations .....	62
4.3.3. COP results .....	64
4.4. System energy analysis .....	66
4.4.1. For a single compressor scenario (the first and the third day).....	66
4.4.2. In a dual-compressor scenario (the second and the fourth day).....	69
5. Recommendations and future work .....	71
6. Conclusion.....	73
Summary .....	76
Bibliography.....	79
Attachments.....	85

## 1. Introduction

Climate change poses a significant threat to the future of our planet, mostly caused by the continuous consumption of fossil fuels to meet the energy demands of residential and commercial sectors. The adoption of renewable energy not only serves as a strong response to the effects of global warming but also facilitates the advancement of energy optimization. Embracing renewable energy solutions, humanity showcases a profound commitment to preserving the environment for upcoming generations, while also positioning ourselves to potentially reap the advantages of reduced energy costs [1]. The European Union (EU) has emphasized the importance of energy efficiency and renewable energy in its strategic plan for sustainable development, recognizing the various challenges associated with this goal. The EU Emission Trading Scheme (ETS) serves as evidence of the EU's commitment to reducing emissions, particularly in the domains of electricity generation and large-scale industrial activities [2]. Within this context, the International Energy Agency's 2012 report highlighted the diverse heating and cooling demands across the EU's 27 nations, pinpointing a significant demand for low exergy heat, particularly between 60 °C and 100 °C. Notably, these requirements are prevalent in sectors like the pulp, paper, food, and tobacco industries. Instead of resorting to fossil fuel combustion, a more sustainable and efficient alternative lies in the adoption of heat pump technology.

Heat pumps, already recognized for their pivotal role in the heating and cooling of homes, have seen an impressive uptake. Between 2010 and 2015, sales figures for electrically driven heat pump units in the EU touched approximately 800.000 units annually [3]. This trend underscores the potential of heat pumps in electrifying heat, presenting a viable alternative to traditional electrical heating. Their inherent efficiency and reduced carbon footprint lend heat pumps a competitive edge [4]. Furthermore, in the broader landscape of energy consumption, refrigeration emerges as a dominant player. Serving a plethora of industries, from food and beverages to chemicals, refrigeration's utility in processes ranging from cooling to environmental conditioning is undeniable.

The core objective of this study is to conduct a thorough energetic assessment of a solar-assisted heat pump with the intention of furthering sustainable heating applications. This exploration delves deep into system efficiency and potential energy losses under various conditions: when operating with a single compressor versus two, and comparing the impact of insulation versus its absence.

All experiments were conducted at the Hungarian University of Agriculture and Life Sciences, Hungary, specifically during the summer season (on four distinct days in the month of July 2023). My ultimate goal is to engineer a setup that minimizes energy losses and to pinpoint areas for potential system enhancements. I hypothesize that mitigating system losses becomes increasingly challenging when both compressors are in operation. Furthermore, it is predicted that an insulated system may exhibit a smaller amount of energy loss relative to an uninsulated counterpart and that the operational loss tends to escalate when operating two compressors. Leveraging the CoolPack software, we theoretically calculated the Coefficient of Performance (COP) and juxtaposed it with experimental measurements. As anticipated, the real-world COP values trended lower, reflecting inherent system losses and the limitations of measurement precision.

This thesis starts with a review that is split into two parts: the initial section shines a light on the diverse applications of heat pumps, emphasizing their unique adaptability and efficiency across various classifications, additionally, it provides valuable insights into the current challenges encountered within the field. The second section provides a detailed analysis of refrigeration cycles, focusing on the functions of system components, exploring the environmental consequences, and conducting a comprehensive exploration of the thermodynamic intricacies that enhance the efficiency of the system. Transitioning to the “Materials and methods” chapter, a thorough outline of the tools, instruments, and experimental setups used in the research is provided. The central focus of the thesis lies in the “Results and discussion” section, where a comprehensive presentation of our findings is presented. In this context, the data undergoes a process of parsing and deliberation and ultimately leads to the generation of conclusive conclusions that reflect the fundamental aspects of our study.

## **2. Literature review**

### **2.1. Introduction to the literature review**

The increasing concern over the environmental impact of non-renewable energy sources has triggered a growing demand for cleaner and more sustainable alternatives. Among these alternatives, refrigeration machines and heat pumps have emerged as pivotal solutions, serving a wide range of purposes. They play a crucial role in maintaining comfortable indoor environments, ensuring the preservation of perishable goods, and facilitating diverse industrial processes. One key advantage of heat pumps lies in their ability to efficiently reduce primary energy consumption through effective heat recovery. As a result, they have garnered significant attention as highly attractive energy conversion devices within the industrial sector.

In the first part of my literature review, I will describe the several fields of endeavor in which heat pumps shine, demonstrating their adaptability and efficiency based on their classifications. Then in the second part, I describe the fundamental aspects of the refrigerant cycle, shedding light on its distinctive characteristics, my focus begins with an exploration of the underlying technology and an in-depth examination of the main component definitions within the system. I proceed then to analyze the thermodynamic behavior of the cycle, unraveling its intricacies and highlighting its efficiency. Finally, I highlight the environmental impact and we address the challenges and potential improvements that lie ahead, identifying the key areas where advancements can be made to optimize the refrigerant cycle and present common software used for this purpose.

### **2.2. Heat pumps classifications and their applications**

#### **2.2.1. Air source heat pumps**

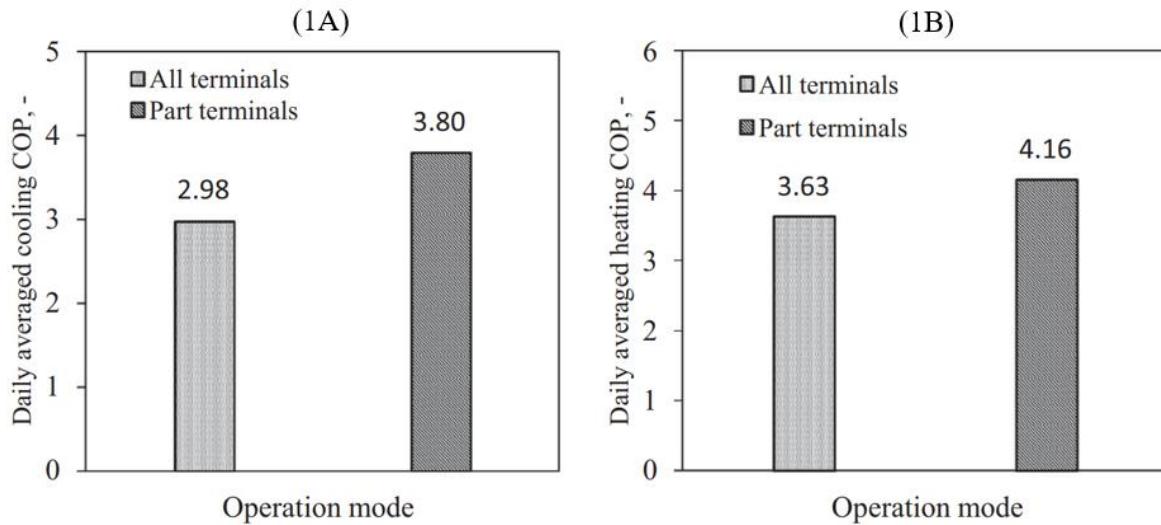
Air source heat pumps (ASHPs) are multifunctional systems that can be used for both heating and cooling by transferring heat energy from the surrounding air to the dedicated area. They can perform their role by pushing heat from low to high temperatures, therefore working against the laws of thermodynamics. Due to their reversible functioning, these setups bring the air's heat energy inside so it can be used for activities like space heating, cooling, and domestic hot water generation. ASHPs can be used in combination with other heating appliances such as air handlers, radiators, and underfloor heating systems to maximize heat distribution [5].



In a typical installation, an ASHP can increase the heat output of a single kilowatt-hour of electricity by a factor of four. These systems perform best in well-insulated buildings with a flow temperature of 30 to 40 degrees Celsius. ASHPs with a flow temperature of up to 80°C can provide full central heating, although at the sacrifice of efficiency [6].

While ASHPs have many benefits, their performance can vary significantly over the annual cycle due to fluctuations in external temperature. This variability becomes a drawback during colder periods when ASHPs provide less heat when it is most needed. To maintain comfortable indoor conditions during such times, supplementary heat from other sources, often resistance heaters, is required [7]. Resistance heating thermal storage methods, which involve storing heat in high-density ceramic bricks within an insulated container as a modern example, offer an efficient alternative to ASHPs [8].

As can be seen in Figure 1, the thermodynamic efficiency of air source heat pump systems can decrease if the air temperature drops during the heating season or rises during the cooling season [9, 10].



**Figure 1.** Daily average Coefficient of Performance (COP) of air source heat pump (ASHP) systems: (1A) In the summer, (1B) In the winter [10].

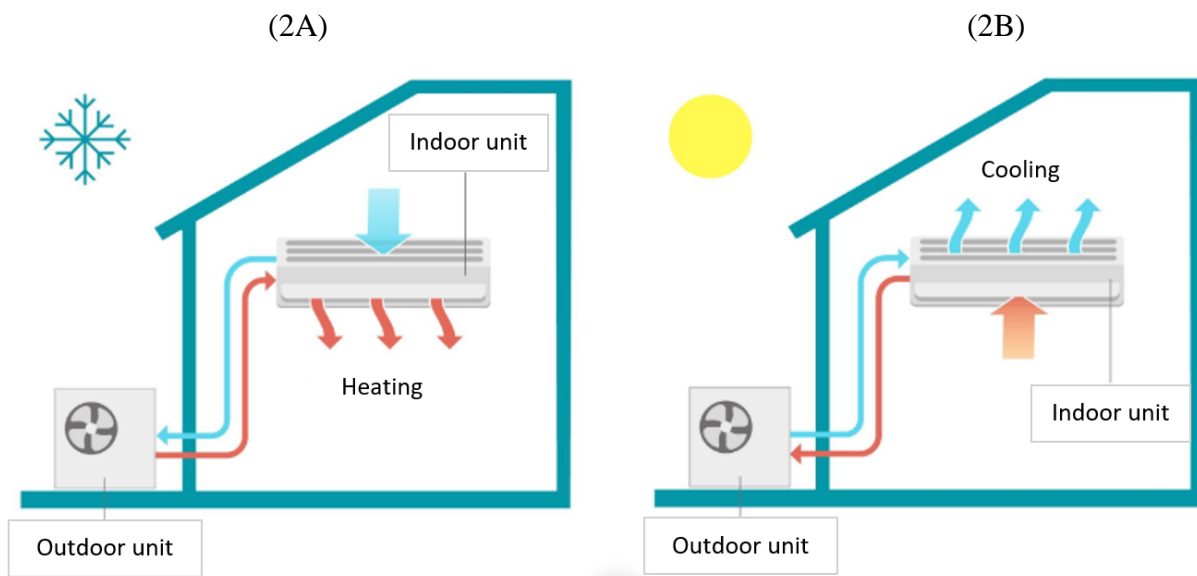
For an ASHP system with various interior terminals and on average cooling and heating days, the average daily COP is displayed in Figure 1. When both the cooling and heating modes are active, the COP values are 2,98 and 3,63, respectively. However, the COP values increase to 3,80 for

cooling and 4,16 for heating when only a subset of terminals is in use. It is important to bear in mind that turning fixed-speed compressors on and off frequently can degrade system performance. Therefore, improving the system's performance necessitates a better compressor control technique.

ASHP can be categorized into two types, air-to-air, and air-to-water heat pumps, depending on the heat exchange process as explained below:

#### 2.2.1.1. Air-to-air heat pumps

In contrast to air-to-water heat pump systems, which are used to warm or cool water, air-to-air systems heat or cool the air directly in the room or building (Figure 2). Therefore, air-to-air heat pump systems often have air handling units, blowers, or fan coil units as part of their indoor equipment. Similar in appearance to commonplace home air conditioners.



**Figure 2.** Schematic illustration of an air-to-air heat pump system: (2A) Heating mode, (2B) Cooling mode [11].

Numerous European countries have investigated the economic feasibility of air-to-air heat pumps [12], providing two to five times as much heat as they consume in energy, air-to-air heat pumps are the most cost-effective alternative to traditional heat pumps [13].

The market is saturated with hundreds of models of both ducted and ductless air source heat pumps, the two primary types of air-to-air source heat pumps. Ducted heat pumps, replacing traditional HVAC (Heating, Ventilation, and Air Conditioning) systems, deliver air through ducts with an interior unit connected to a remote compressor. These are often centrally controlled systems, with compact versions handling two to four rooms [14]. Offering benefits like concealed ductwork, simple temperature adjustments, and enhanced air quality due to integrated filters and purifiers, they stand out as efficient, cost-effective, and user-friendly solutions [15]. On the other hand, ductless or mini-split heat pumps, which avoid the need for ducting, are a preferable choice when ductwork installation is impractical or expensive. They feature straightforward setups, with indoor units connecting to an outdoor counterpart [16]. With benefits like energy efficiency, precise temperature control, improved air quality, and silent operation, they're apt for homes without existing ducts or spaces with fluctuating temperature needs [17].

#### **2.2.1.2. Air-to-water heat pumps**

Space heating and household hot water can both benefit from the air-to-water heat pump system's ability to convert the thermal energy in ambient air into usable heat [18]. Using a power-driven fan, they bring in fresh air from the outdoors. By blowing hot air over a coil of liquid refrigerant (the evaporator), that substance is vaporized. The gas is subsequently heated by a compressor, the heat pump's main source of electrical consumption. A second heat exchanger (the condenser) is utilized to transfer the heat from the hot refrigerant gas to a closed water loop that can subsequently be used for space heating and/or hot water production. The cooled refrigerant returns to the evaporator via an expansion valve. This cycle occurs over and over again [19]. In a study conducted in Hungary, it was found that using air-to-water heat pumps can result in a 30% cost reduction in specific conditions [20].

Although air-to-water heat pump devices are a viable option for replacing or integrating gas boilers and saving the environment from greenhouse gas emissions [21], planners may find it difficult to accurately assess the systems' seasonal performance. As the ambient temperature varies constantly throughout the year, the efficiency of an air-to-water heat pump varies greatly from one season to the next. Heat pump performances (i.e. their energy consumption) over the whole heating or cooling season are heavily influenced by several external elements, such as the changeable building thermal load, the outer environment, and the type of heat pump's control system. Since

heat pumps operate at nominal conditions for only a portion of the season, it is essential to take into account their behavior at partial loads when calculating their seasonal efficiency [22].

### **2.2.2. Water-source heat pumps**

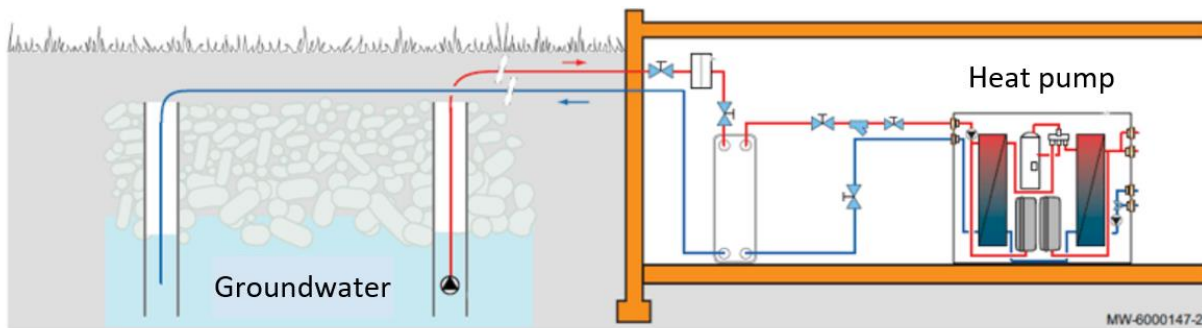
In response to rising demand, water-source heat pump systems have been demonstrated to be preferable to traditional air-source heat pump systems in terms of energy efficiency and reliability [23]. Water-source heat pumps utilize water sources as a thermal energy supply for heating and cooling, which has gained attention as an efficient approach to energy production for buildings and industrial applications [24]. For a long time, people all over the world have been utilizing the thermal energy of water sources for use in massive heating and cooling infrastructure. Water from rivers, raw water, oceans, lakes, and even the ground is used [25]. A study cited in [26] employed waste heat from a power plant to warm a greenhouse in South Korea, the utilization of high-temperature wastewater led to a 19% reduction in the energy needed to heat the greenhouse. Another notable instance is the case of a hotel located in Wuhan, China, which effectively reduced its air conditioning's energy consumption by 43% by extracting water from a depth of 23,6 meters below the ground [27].

Water source heat pump performance can be enhanced by keeping the water temperature lower than the surrounding air during the summer and higher during the winter. In the summer, free cooling allows the water supply to be used for cooling purposes using only pumps without the heat pump compressor if there is an abundance of cold water. These energy benefits can also help lessen carbon emissions and fine dust, while the elimination of the need for a cooling tower and boiler flue in buildings thanks to the use of a water source system maximizes the interior floor area for other purposes. As with the boiler flue, removing the cooling tower from the roof makes room for greenery and a resting place inside the building [28].

Water-source heat pump systems outperform air-source heat pumps due to water's heat transfer qualities. The source, destination, and medium the heat pump utilizes to absorb or reject heat in each place establish their basic heating types, the heat transfer appliance for both heat exchangers can be air, liquid (water or glycol), or a combination of these two [9].

### 2.2.2.1. Water-to-water

Water-to-water heat pumps (Figure 3) employ water as both the heat source and heat sink during the heat exchange procedure. These systems are frequently utilized for various purposes, including air conditioning for enhanced comfort, precooling of fresh produce or flowers, and cooling process fluids naturally in industries such as chemical, pharmaceutical, and food processing when cold utility is required. Additionally, they are employed for heating water directly, such as for heating process fluids like cleaning solutions in industrial washing machines, drying agricultural products, and regenerating desiccants. This latter application is particularly useful for managing the latent cooling load when hot utility is needed [29].



**Figure 3.** Schematic example for a water-to-water heat pump [30].

Groundwater is usually from 8 to 15 degrees Celsius. This is enough to provide high-efficiency heat pump energy and hot water and it requires well drilling and preparation. The operation of a water-to-water heat pump necessitates the establishment of both production and sinking wells. The production well water is subsequently circulated back to the sink well by the heat pump. The choice of aquifer location holds significance in this process. It is crucial to consider that surface temperatures tend to fluctuate, which can adversely affect nearby water bodies in terms of pollution [31]. The cost of drilling a borehole to reach the groundwater can range widely, depending on factors like the depth of the earth and the type of ground that must be traversed. As a result, there is a growing need for groundwater that is putting pressure on the established groundwater industry [32].

### 2.2.2.2. Water-to-air

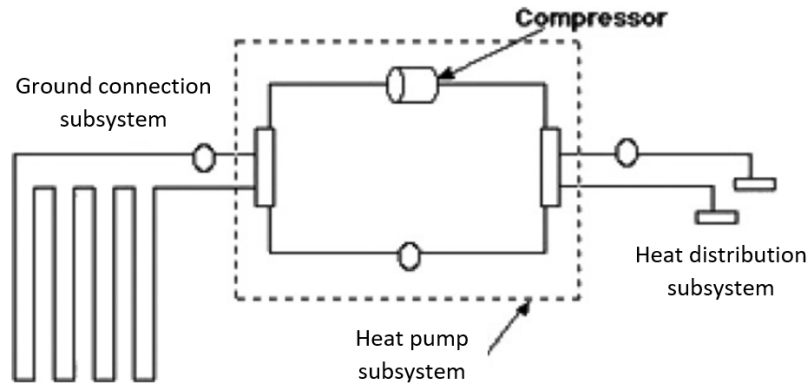
Water-to-air heat pumps transfer heat energy from underground water to the indoor air distributed through a building's ductwork. By utilizing the temperature difference between hotter and colder

materials, during winter, water-to-air heat pumps provide forced-air heating, while in summer, they supply central air conditioning. These heat pumps are specifically compatible with forced-air HVAC systems, whereas water-to-water heat pumps work with hydronic radiant HVAC systems like radiators, hot water baseboard heaters, and radiant floor heating. Water-to-air heat pumps offer various applications, including comfort air conditioning, and precooling of perishable goods. It is also utilized in other industries, including chemical, pharmaceutical, and food processing. Additionally, they provide hot utility for space air heating, drying clothes, and regenerating desiccants.

The heat interactions in the evaporator and condenser can involve multiple sources and sinks, allowing for the simultaneous generation of multiple cold and/or hot utilities and offering flexibility to maximize the benefits of a heat pump system [33].

### **2.2.3. Ground source heat pumps**

Ground-source heat pumps (GSHP), which have been extensively utilized in various regions around the world such as in North America and Europe, have proven to be a reliable and eco-friendly heating solution for over two decades. While their initial installation costs are higher compared to conventional systems, they boast minimal maintenance expenses. Unlike ASHPs, GSHPs are more energy efficient due to their ability to extract or release heat from the earth, which maintains moderate temperatures throughout the year. This characteristic enhances the effectiveness of heat transfer, as opposed to relying on the air, which experiences colder winters and hotter summers [34]. By employing GSHPs, cooling energy consumption can potentially be reduced by 30% to 50%, while heating energy can be decreased by 20% to 40% [35]. GSHP systems have gained significant popularity worldwide in residential and commercial buildings, primarily due to their appealing benefits in terms of energy efficiency and environmental impact. These systems have witnessed extensive utilization in various types of buildings, including both residential and commercial structures. Recent estimates indicate continuous global growth in GSHP system installations, with an annual increase ranging from 10% to 30% [36].



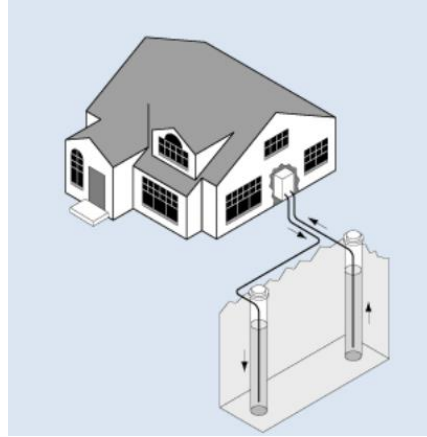
**Figure 4.** Ground heat pump cycle [34].

A typical GSHP system (Figure 4) consists of three key components: (1) a ground connection subsystem, (2) a heat pump subsystem, and (3) a heat distribution subsystem. The ground connection subsystem enables the transfer of heat between the ground and the system, serving as a vital link in the overall heat exchange process. The heat pump subsystem is responsible for extracting heat from the ground or releasing it into the ground, depending on the desired heating or cooling operation. Lastly, the heat distribution subsystem ensures that the generated heat is effectively distributed throughout the building to provide comfortable indoor temperatures [36].

Several aspects must be taken into account in order to select the optimal system for a given installation, including the geology and hydrogeology of the subsurface, the extent and usage of any potential heat sources on the surface, such as mines, and the heating and cooling characteristics of the building(s) in question [34].

#### **2.2.3.1. Open systems**

The simplest and most basic GSHP systems are open-loop systems like the one seen in Fig. 5, which have been in use since the 1970s. Groundwater is pumped up to the heat pump for use as the heat carrier in these setups. The water is either re-injected into the well or released into a nearby body of water. These setups can only function with access to a large quantity of clean, shallow groundwater. Municipal restrictions can prevent the installation of open-loop systems due to their impact on community groundwater [37].

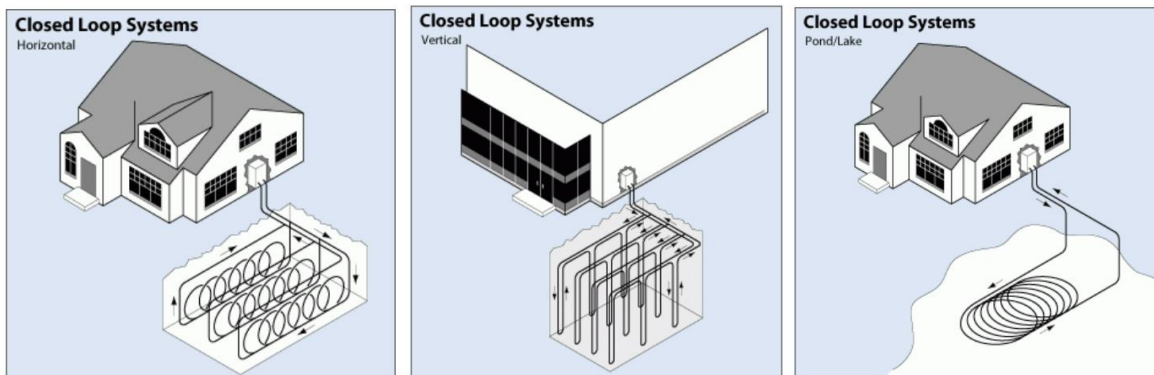


**Figure 5.** Open-loop system [38].

Groundwater runs freely underground and works as a heat source/sink and a medium to exchange heat with the solid earth in this type. Open systems use groundwater wells to draw or inject water from subsurface aquifers. Two wells are needed to remove and re-inject groundwater. Open systems can use powerful heat sources cheaply. However, groundwater wells need upkeep, and open systems are limited to appropriate aquifers [39].

#### 2.2.3.2. Closed systems

In closed systems, heat is transferred from the earth to the heat pump (or vice versa) via heat exchangers buried underground in a horizontal, vertical, or oblique orientation (Figure 6). It is a closed system since the heat carrier is isolated from the rock/soil and groundwater by the heat exchanger's wall [34].



**Figure 6.** Examples of closed-loop systems: (6A) Horizontal, (6B) Vertical, (6C) Pond/Lake [39].



Digging a 4-5 ft trench instead of a deep well makes the horizontal loop cheaper. It takes more acreage because shallow ground temperatures vary seasonally. System size, climate, soil/rock thermal properties, and loop type determine pipe length. A typical horizontal loop requires 2000-3500 ft<sup>2</sup> per ton.

Vertical boreholes are 150 to 220 ft deep per ton. The vertical loop requires 200 – 400 ft<sup>2</sup> of ground surface area, making it more practicable for small properties, but also increases system installation costs due to drilling.

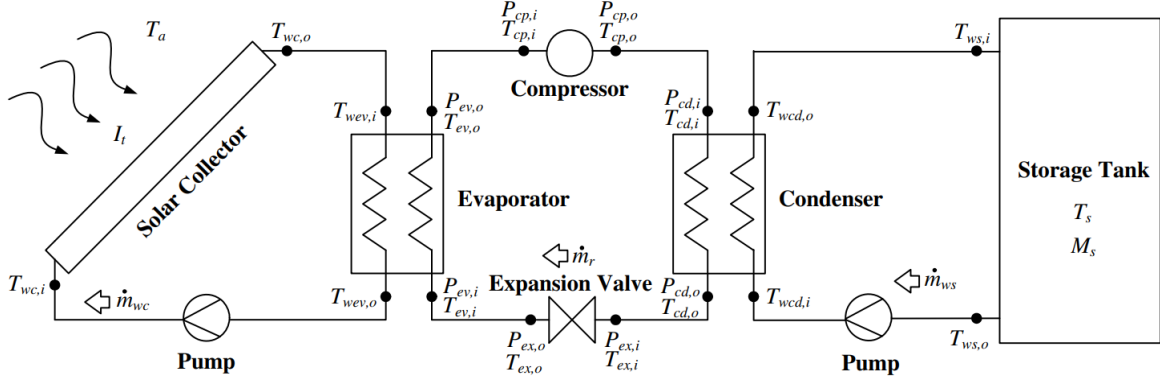
Lake or pond loops submerge the ground loop. This concept requires minimal digging and is cost-effective if a suitable body of water is available. Direct exchange systems heat the ground loop using refrigerant. Without a pump, such systems need a longer copper tube and more refrigerant [38].

### **2.3. Solar-Assisted Heat Pump**

As highlighted earlier, the industry today boasts a diverse range of heat pumps. Given the limited scope of the available literature, the subsequent section provides a concise overview of one of the most recent advancements: Solar-Assisted Heat Pumps (SAHPs).

#### **2.3.1. Technological methods and their applications**

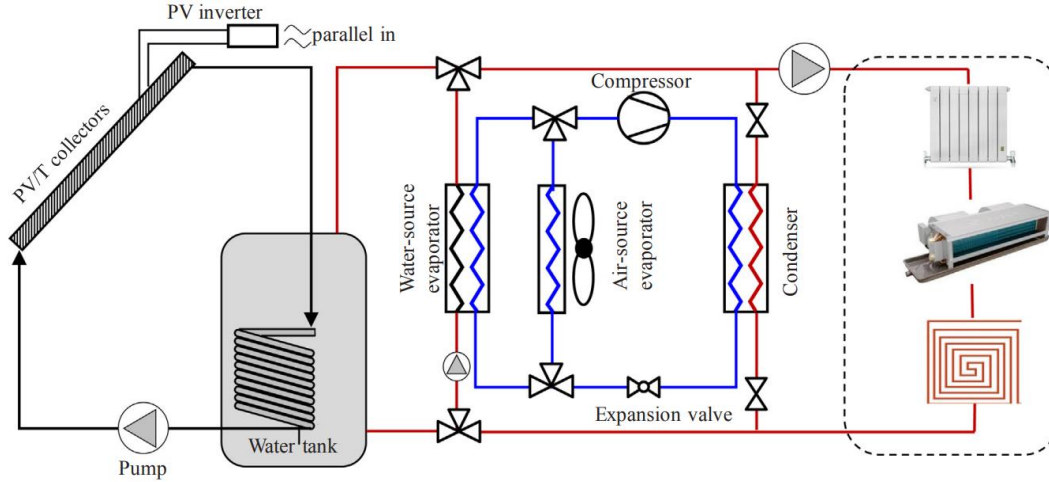
Beyond the commonly referenced heat pump sources; air, water, and ground, the Solar-Assisted Heat Pump (SAHP) stands out as an innovative alternative. This system excels at both cooling and heating by harnessing the sun's energy to facilitate enhanced heat exchange, boosting overall efficiency. Integrating solar panels, typically solar thermal panels, the SAHP captures solar energy to assist in the heating or pre-heating process. This captured energy can pre-heat the refrigerant, reducing the energy required by the heat pump's compressor and other components. In a study conducted by [40], a comparative assessment of Flat-Plate Collector (FPC) data was undertaken with a focus on its applications for domestic hot water (DHW). Serving as a real-world example for this investigation was a laboratory at Szent Istvan Campus, located in Gödöllő, Hungary. Practical findings from this case study highlighted that the model utilized achieved a commendable 69% solar fraction, corresponding to an annual solar yield of 510 kWh. It's noteworthy to mention that such technologies hold potential for integration with heat pumps, a domain that has seen significant advancements over the past two decades.



**Figure 7.** Experimental layout of a solar-assisted heat pump [41].

Figure 7 shows a detailed experimental layout of a SAHP. The liquid used for heat transfer in this setup as referenced in [41], is water. This medium circulates through the solar panel, facilitating the transfer of heat from the solar collector to the evaporator and subsequently from the condenser to a storage tank. While water is the chosen fluid in this experiment, other mediums such as glycol, and air, can also be employed to serve a similar purpose, depending on the specific requirements and environmental conditions of the application.

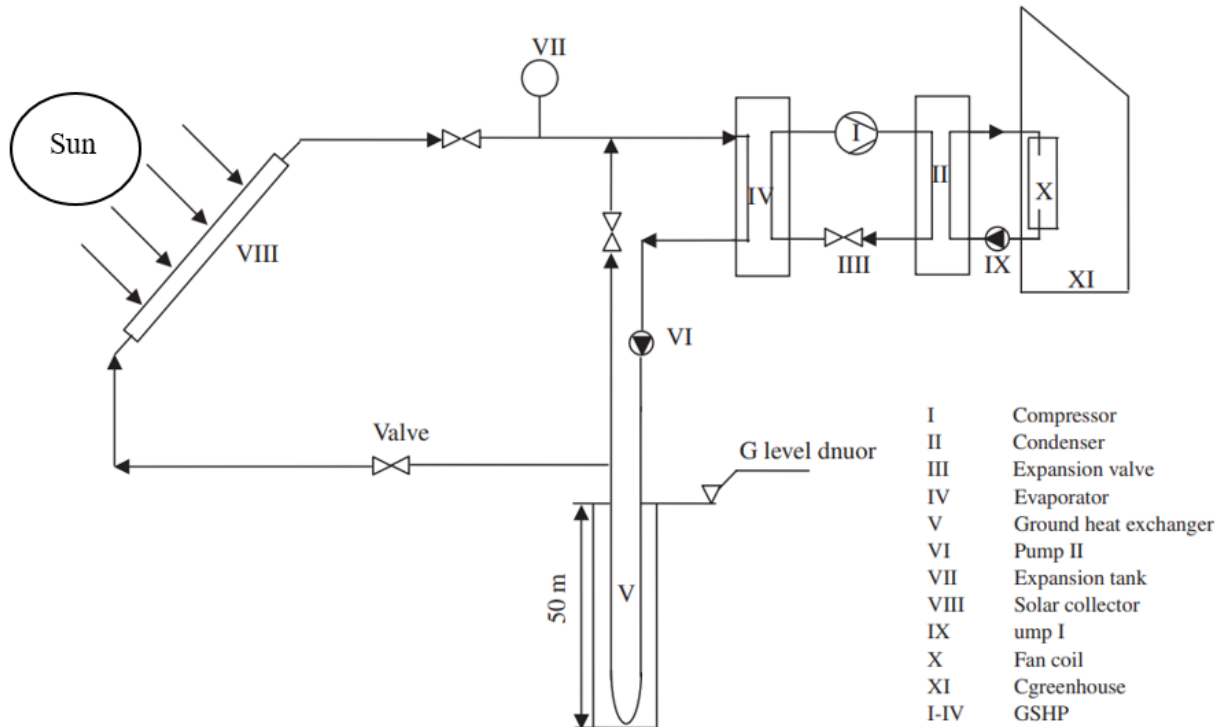
Besides the thermal panels, hybrid solar panels, also known as Photovoltaic/thermal (PV/T) collectors, are advanced devices designed to concurrently harness solar energy for both electricity and heat generation. They are perceived as a viable, eco-friendly energy alternative, and due to their dual functionality, they are particularly advantageous for rural locations with ample space for deployment. On the other hand, flat plate PV/T collectors, as studies suggest in [42], offer superior energy yield per unit surface area compared to standalone PV panels or traditional collectors. The thermal energy captured by these hybrid panels can be channeled for various purposes, including space heating, water heating for domestic use, and drying processes.



**Figure 8.** Schematic representation of a standard dual-source SAHP [43].

Solar-assisted heat pumps are classified based on their integration with PV/T collectors into two types: direct expansion solar-assisted heat pumps (DX-SAHP) and indirect expansion solar-assisted heat pumps (IDX-SAHP). Notably, the IDX-SAHP, which uses water as its medium for energy transmission and storage, is extensively researched and implemented. Figure 8 depicts a standard configuration of a dual-source IDX-SAHP. Typically, such a system is equipped with two distinct evaporators: one that draws heat from the water-based PV/T or water tank, and another that harnesses heat from ambient air as an additional source [43].

The recent advancements in technology have enabled the integration with GSHPs, leading to the development of what is termed Solar-Assisted Ground Heat Pumps (SAGSHPs). A detailed analysis was undertaken on the energy and exergy assessments in Turkey of SAGSHPs designed specifically for greenhouse heating (SAGSHPGHS). To avoid water freezing during operation and especially in cold seasons, a solution consisting of 10% ethyl glycol by weight was utilized. R-22 served as the working fluid, with the refrigerant circuit intricately designed using closed-loop copper tubing, as depicted in Figure 9.



**Figure 9.** Solar-assisted ground source heat pump (designed for heating a greenhouse) [44].

Using the setup in Fig. 9 an experimental study was conducted on *Cucumis sativus* cv. Pandora F1 from December 16, 2003, to March 31, 2004, throughout this period, the quality of the product was significantly enhanced due to optimal climatic conditions. The Coefficient of Performance for the Heat Pump ( $COP_{HP}$ ) ranged between 2,00 and 3,125, As for exergy efficiency, the GSHP unit achieved 71,8%, and when evaluating the entire system based on a product-to-fuel ratio, the efficiency stood at 67,7% [44].

### 2.3.2. Technological hurdles in SAHP development

Properly integrating solar thermal components with heat pump systems presents a nuanced challenge due to the inherent complexities of integration. The inconsistency of solar radiation, influenced by climatic shifts and diurnal cycles, adds another layer of difficulty, prompting researchers to explore advanced control strategies for optimal operation under fluctuating solar conditions. Further, the goal is not only to harness the sun's energy but to do so efficiently, demanding precise calibration for system optimization in real time. The longevity of SAHPs, especially when exposed to the relentless outdoor elements, remains a top priority, driving investigations into durable materials and protective innovations. While these systems offer a

promising sustainable energy solution, their initial setup costs can be a deterrent, necessitating research into designing both cost-effective and efficient systems. Environmental considerations also play a pivotal role, with initiatives focusing on minimizing SAHPs' environmental footprint, whether by curtailing refrigerant emissions or by adopting eco-friendly refrigerants.

Finally, while SAHPs prove beneficial for individual households, their application on an industrial scale introduces additional complications. Addressing this, ongoing efforts are centered on creating modular SAHP solutions that can be seamlessly scaled up [45].

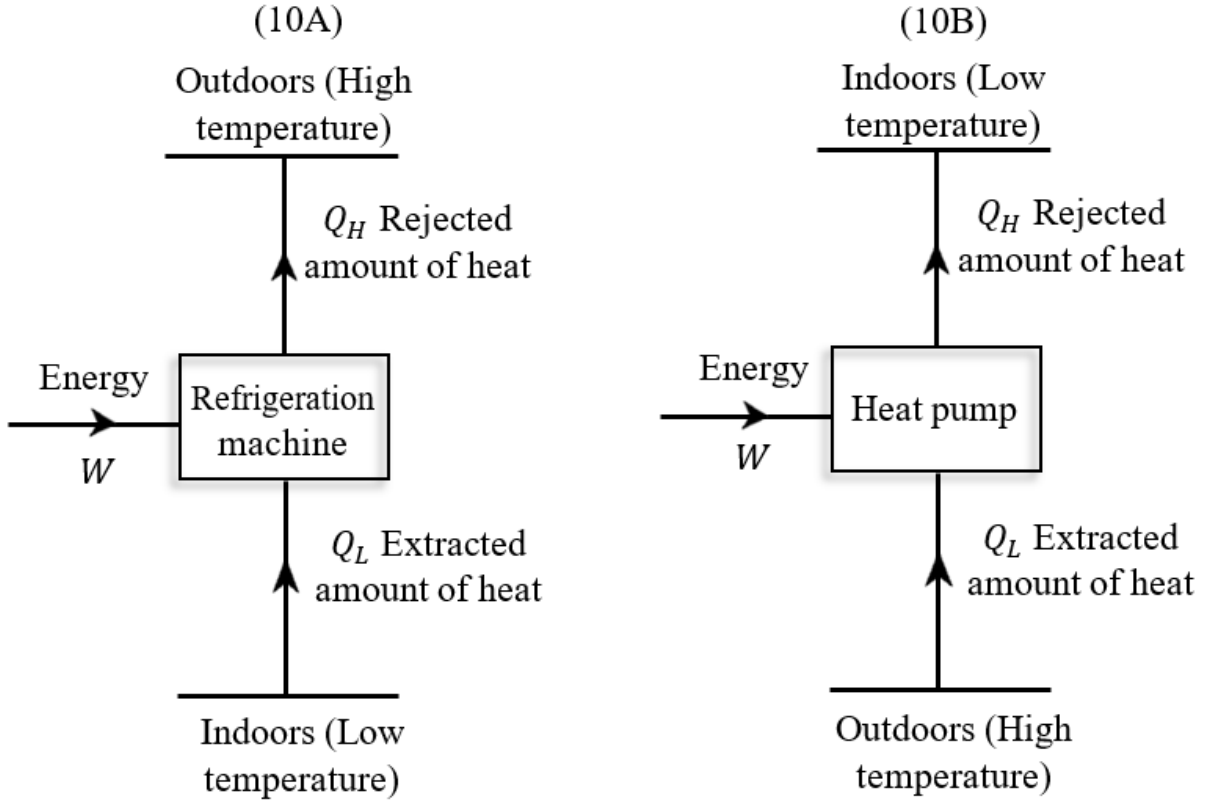
In conclusion, although the scope of this thesis limited the coverage of all types and applications of heat pumps, the previous literature provided a comprehensive and well-oriented overview of their applications and classification. The forthcoming section will delve into a detailed explanation of the working methodology of a typical heat pump, further enhancing our understanding of this technology.

## **2.4. Heat pumps and refrigeration machines technology**

### **2.4.1. Definition**

In the field of thermal energy management, heat pumps, and refrigeration units represent novel technologies [46]. These systems make use of the laws of thermodynamics to effectively and efficiently heat or cool a given area. Heat pumps are adaptable heating appliances that can draw heat from the outdoors, even in cold climates, and move it indoors. Space heating, water heating, and air conditioning may all be done in an environmentally responsible manner. With the help of these products [47].

Cooling and freezing items, condensing vapors, preserving climatic conditions, and cold storage are just a few of the many uses for refrigeration machines. They are built for chilling and freezing, and are thus indispensable in the preservation of perishable goods, maintaining comfortable indoor environments, and the facilitation of numerous industrial processes [48]. They work in the same way as heat pumps, but their primary function is to reduce the temperature of an enclosed room by expelling heat from the area [49], sketch in Figure 10 provides a global overview of this technology.



**Figure 10.** Schematic illustration of: (10A) Refrigeration machine (10B) Heat pump system.

By applying the first principle of thermodynamics for this system:

$$\Delta U_{Cycle} = W_{Cycle} + Q_{Cycle} = 0 \quad (1)$$

$$W + Q_L + Q_H = 0 \quad (2)$$

The rejected heat can be written as follows:

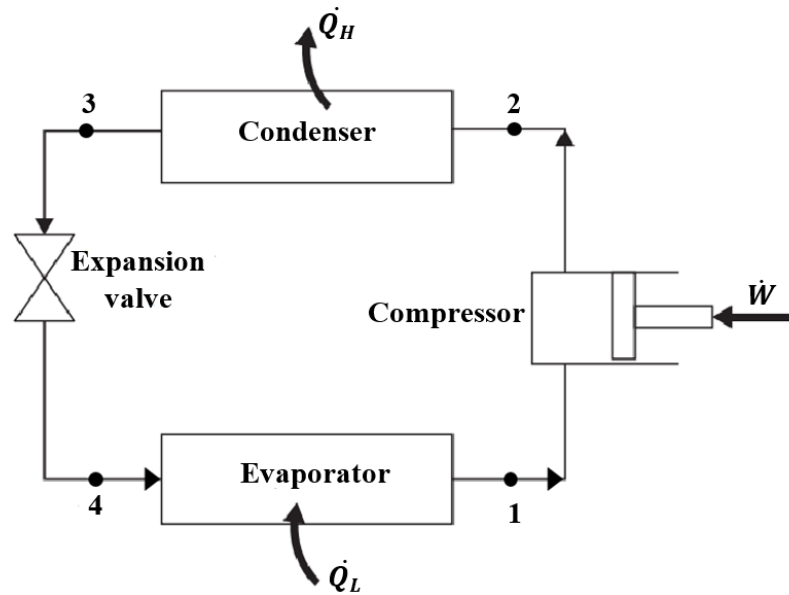
$$|Q_H| = |Q_L + W| \quad (3)$$

And it represents the desired output for the heat pump.

#### 2.4.2. Main components

Refrigeration and heat pump machines have four primary components. The compressor makes the refrigerant circulate through the cycle. The condenser removes heat from the refrigerant, cooling it and turning it into a high-pressure liquid. The expansion valve lowers refrigerant pressure and temperature. The evaporator converts heat from the environment into a low-pressure gas,

completing the cycle. The system is represented in Figure 11 below followed by an explanation for each component and its role.



**Figure 11.** Schematic drawing for a refrigeration cycle.

### Compressor

The compressor represents the heart of the refrigeration system, as it is responsible for increasing the pressure of the refrigerant by reducing its volume. The selection of a compressor is influenced by various factors such as efficiency, reliability, size, and cost. Table 1 highlights the most common compressor types and their notable features [50]. When selecting a compressor, it is important to think about its operational characteristics and aspects, including the number of stages, cylinder action, compressor size and working speed, cylinder arrangement, valve design, drive type, capacity control type, lubrication type, and sealing type.

**Table 1.** Main types of compressors [50].

Type	Model	Capacity (kW)	Refrigerant	Application
Reciprocating	– Hermetic – Semi hermetic – Open	0.1/30 30/250 250/50	R134a R404A R407A R407C R717 R744	Industrial and commercial refrigerators, low temperature industrial refrigeration
Vane	Hermetic	0.75/3	R407C R410A R744	Small refrigerators, portable air-conditioning, split systems
Scroll	Hermetic	3.5/90	R407C R410A	Low and medium size air-conditioning
Screws	– Semi hermetic – open	80/8000	R407C R134a R717	Medium and large power air conditioning. Industrial refrigeration
Single screw	– Semi hermetic – Open	100/500	R134a R410A	Medium and large power chillers for commercial and industrial climatization

### Condenser

Condensers are an essential component in refrigeration cycles; they are responsible for transferring heat away from the refrigerant toward the surrounding environment. As a result of this, the refrigerant can change from the phase of superheated vapor (high-pressure vapor at a high temperature) to a high-pressure saturated or totally liquid phase. The heat can be transferred through a variety of mediums, such as air, water [51], or ground [52], depending on the availability of the cold source, the limitations imposed by space, and the level of efficiency that is required.

The efficiency of a condenser significantly affects the overall performance of a refrigeration system. A well-designed condenser facilitates efficient heat transfer and ensures proper condensation of the refrigerant [53].

### Expansion valve

The expansion valve plays a pivotal role in the vapor compression cycle, which divides a refrigeration system into two pressure sides, known respectively as the high-pressure side and the



low-pressure side [54]. In the context of the expansion process, an expansion valve may take various forms such as a valve, an orifice plate, or a capillary tube [55]. It adjusts the amount of refrigerant that flows through the system based on the quantity of cooling work being done by the evaporator. Since expansion devices base their operations on the principle of expanding the refrigerant through a throttling process in the vast majority of applications, the enthalpy of the refrigerant has the potential to remain constant during expansion [54].

### Evaporator

Evaporators are heat exchangers that work on the same principle as the condensers but in the opposite direction of the heat flow. They represent the main purpose of refrigeration installation, as they are the source of cold production. In the evaporator of a refrigeration system, a low-pressure vapor of a cool refrigerant is brought into contact with the medium or substance that needs to be cooled (also known as a heat sink), this causes the refrigerant to absorb heat and produce a low-pressure saturated or superheated vapor [55].

### **2.4.3. Refrigerants**

A refrigerant is a chemical substance that acts as a heat carrier in the heat pumps, and it represents the lifeblood of the system. During the cycle, the refrigerant undergoes reversible phase transitions: initially from a low-pressure gas to a high-pressure liquid, and subsequently back to a gaseous state, as it circulates through various components of the system [56]. The core function of the refrigerant is to absorb thermal energy from a designated space, causing its phase transition from a low-pressure gas to a high-pressure liquid. It then transports this absorbed heat to another location, thereby achieving the desired cooling or heating effect, depending on the system's objectives.

Industrial refrigeration systems are particularly versatile and capable of operating within a broad temperature spectrum. While some applications may require evaporating temperatures as elevated as  $15^{\circ}\text{C}$ , industrial systems can also accommodate extreme low-temperature conditions, reaching down to approximately  $-60^{\circ}\text{C}$  or even  $-70^{\circ}\text{C}$  [57]. This adaptability makes industrial refrigeration systems invaluable in a diverse range of sectors, from food preservation to chemical processing and beyond.

### Classification of refrigerants and environmental impacts

More than 60 new refrigerants were commercialized for use either in new equipment or as service fluids (to maintain or convert existing equipment) in the past four years [60]. Different types of refrigerants are distinguished from one to another based on their chemical structure, safety potentials, and ecological footprint. In the following table, I present a detailed breakdown of commonly used refrigerants, categorizing them based on their chemical composition and corresponding safety levels [61, 62].

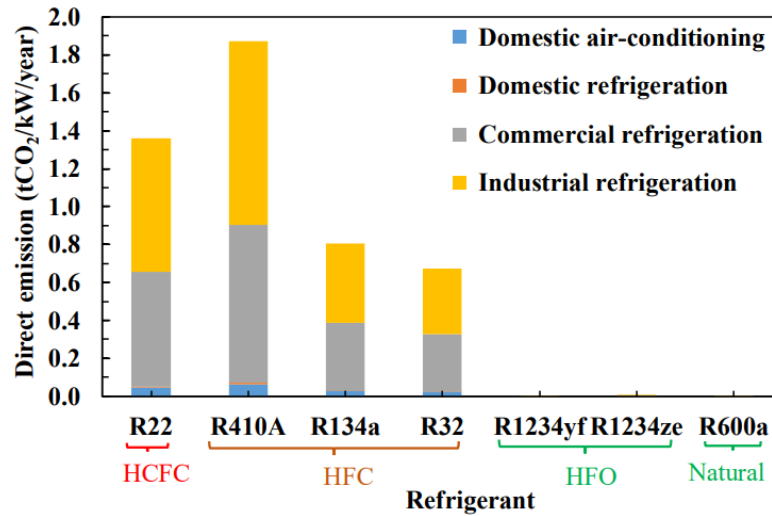
**Table 2.** Chemical and safety classification of commonly used refrigerants.

Chemical category	Commonly used refrigerants	Safety classification
Chlorofluorocarbons (CFC)	R-12, R-11	Class A1
Hydrochlorofluorocarbons (HCFC)	R-22, R-123	Class A1
Hydrofluorocarbons (HFC)	R-134a, R-404A	Class A1
Hydrocarbons (HC)	R-600a (Isobutane), R-290 (Propane)	Class A3
Carbon Dioxide (CO <sub>2</sub> )	R-744	Class A1
Ammonia (NH <sub>3</sub> )	R-717	Class B2
Hydrofluoroolefins (HFO)	R-1234yf, R-1234ze	Class A2L

The safety classification entails two alphanumeric parts, for instance, “B2”, where the first letter refers to toxicity and the second digit to flammability. Below 400 parts per million (ppm), Class A refrigerants are non-toxic, but Class B refrigerants are hazardous. Class 1 refrigerants are naturally non-flammable, Class 2 refrigerants have low flammability, and Class 3 refrigerants are extremely flammable [62].

To mitigate the environmental and safety risks of refrigerants, a multi-tiered system of laws and standards has been established at both international and national levels. These regulations are influencing the choice of refrigerants, leading to the phasing out of environmentally harmful options like certain HFCs, and encouraging the use of “natural” refrigerants [63]. The implementation of stricter laws on ozone depletion potential (ODP) and global warming potential

(GWP) has led to an increased focus on the investigation of environmentally friendly refrigerants [64].



**Figure 12.** A comparative analysis of direct CO<sub>2</sub> emissions per kWh/year among different applications [65].

Figure 12 illustrates the annual CO<sub>2</sub> emissions per kilowatt for different systems. Notably, industrial and commercial refrigeration units are major sources of direct greenhouse gas emissions due to their high leakage rates and large initial refrigerant charges [65]. Moreover, experimental heat pump systems, like the one studied in [66], are showing promise in industrial settings. For example, in the brewing sector, it has been demonstrated that using a dual-source heat pump could slash CO<sub>2</sub> emissions by 60% and reduce energy costs by 10%.

#### 2.4.4. Refrigeration cycle

The Carnot cycle was the first cycle imagined to operate refrigeration and heat pump machines. Carnot cycle is a reversible cycle and it is composed of two isentropic transformations (2→3 and 4→1), and two isotherm-isobaric transformations (1→2 and 3→4) as it is illustrated in the diagram T-S in Figure (13A) [67].

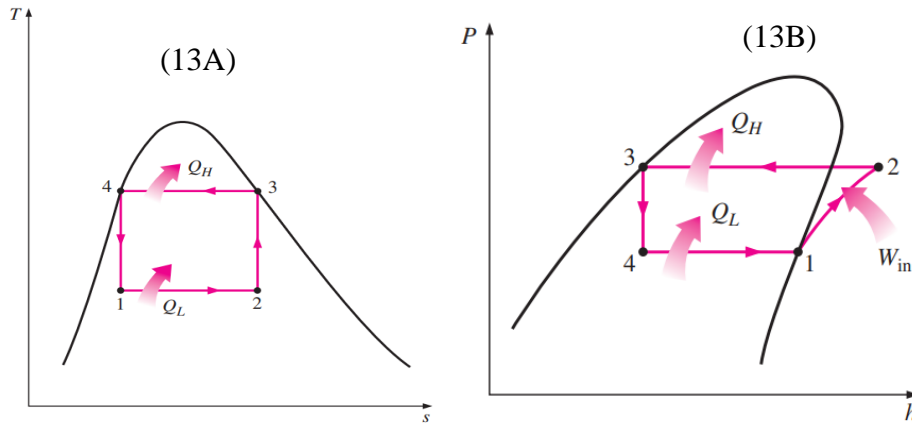
- In the transformation (1→2 and 3→4), we find that the heat is either taken out of the system (at the level of the evaporator) or delivered to a warm spot (at the level of the condenser).
- In the transformation (1→2 and 3→4) in which the compressor and the expansion valve are thermally isolated (no heat transfer with the ambient environment), in this process, the

gas is compressed isentropically until reaches a point of high pressure and temperature, and reducing its pressure and temperature while passing through the expansion valve.

The cycle depicted on the right-hand side (13B) represents the ideal cycle, which encompasses the following key processes:

- Isotropic compression (1→2): This process involves the compression of the refrigerant in an isentropic (reversible adiabatic) manner.
- Constant pressure heat rejection in the condenser (2→3): The refrigerant, at high pressure and temperature, releases heat to the surroundings while maintaining a constant pressure.
- Expansion valve throttling (3→4): The refrigerant undergoes a throttling process by passing through an expansion valve, resulting in a decrease in pressure.
- Constant pressure heat absorption in the evaporator (4→1): The refrigerant, at low pressure and temperature, absorbs heat from its surroundings while maintaining a constant pressure.

These processes constitute the ideal vapor compression refrigeration cycle, which is commonly employed in refrigeration and air conditioning systems [68].



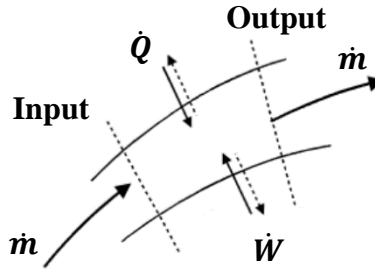
**Figure 13.** Thermodynamic cycles: (13A) Temperature-Entropy (T-S) Diagram of the reversed Carnot cycle, (13B) P-h diagram of the ideal cycle [69].

The ideal or typical vapor-compression refrigeration cycle (13B) overcomes several challenges linked to the reversed Carnot cycle through two modifications: complete vaporization of the refrigerant until reaching the phase of saturated vapor before compression, and the replacement of

the turbine with a throttling device like an expansion valve or capillary tube. These changes eliminate many of the impractical aspects associated with the reversed Carnot cycle.

## 2.5. Energy examination of the system

To examine thermodynamic processes and analyze energy transfers in each part of the system, it is necessary to have a good understanding of the first law of thermodynamics, generally known as the law of conservation of energy.



**Figure 14.** Schematic representation of a control volume (CV).

The area between the input and the output is called the control volume, where the refrigerant can transfer energy with the surroundings, the alteration in energy within this control volume is delineated by the equation (4):

$$\frac{dE}{dt} = \dot{Q} + \dot{W} + \sum_{In}^{out} \dot{m} (h + \frac{1}{2}V^2 + gz) \quad (4)$$

Where:

$\frac{dE}{dt}$ : Energy variation in the control volume [W].

$\dot{Q}$ : The heat transferred in the control volume [W], positive if heat is added, negative if heat is removed.

$\dot{W}$ : The work generated/ received for the control volume [W].

$\dot{m}$ : Net mass flow rate into or out of the control volume [ $\frac{Kg}{s}$ ].

$h$ : Specific enthalpy of the refrigerant [ $\frac{J}{Kg}$ ].

$V$ : Refrigerant velocity [ $\frac{m}{s}$ ].

$g$ : The acceleration of gravity [ $\frac{m}{s^2}$ ].

After making the following simplifications:

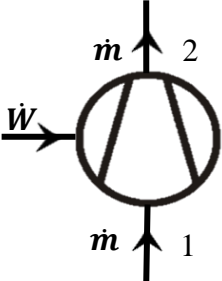
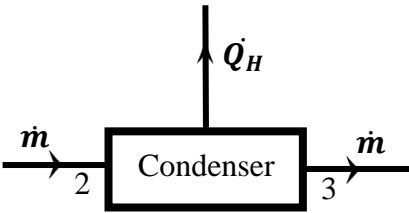

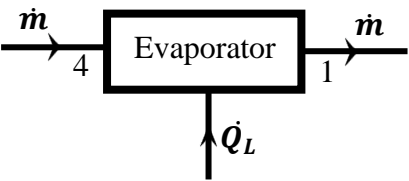
- According to the First Law of Thermodynamics, energy is conserved, meaning  $\frac{dE}{dt} = 0$ .
- Typically, the changes in kinetic and potential energies are negligible when compared to enthalpy ( $\frac{1}{2}V^2 + gz = 0$ ).

For a specified control volume (CV) within the system, Equation (4) can be reformulated as:

$$\dot{Q} + \dot{W} = \dot{m}(h_{out} - h_{in}) \quad (5)$$

These equations have been consolidated for all components of the heat pump and are presented in Table 3 below.

**Table 3.** Energy balance summary for heat pump components.

The component	Schematic illustration	Energy equation	Equation No.
The compressor		$\dot{W} = \dot{m}(h_2 - h_1)$	(6)
The condenser		$\dot{Q}_H = \dot{m}(h_3 - h_2)$	(7)
The expansion valve		$\dot{m}(h_4 - h_3) = 0$ (Since $h_4 = h_3$ )	(8)
The evaporator		$\dot{Q}_L = \dot{m}(h_1 - h_4)$	(9)

Note:

Based on these calculations, we assumed on the equations listed above that the refrigerant was in a steady state and the compressor worked with no heat transfer during operation. The pressure drop is also neglected.

### Vapor quality

The quality of vapor  $x$  is an indicator to describe the state of a two-phase substance, and it is defined as the ratio of the mass of vapor to the entire mass of a vapor-liquid mixture (see equation (10)).

$$x = \frac{m_{vapor}}{m_{vapor} + m_{liquid}} \quad (10)$$

Where  $m$  refers to the mass of the refrigerant [Kg].

Unlike a liquid with a quality of 0%, vapor has a quality of 100%.

Heat pumps and refrigeration machines have long relied on accurate assessments of vapor quality to achieve optimal system performance and the intended results.

### Coefficient of performance (COP)

A heat pump, refrigerator, or air conditioner's efficiency can be measured by its coefficient of performance (COP). It is the ratio of the work (energy) necessary to run a system to the desired output (amount of extracted heat in the case of a refrigeration or air conditioning machine, the amount of rejected heat in the case of a heat pump). If the COP is high, then the system is efficient and consumes less energy [70].

$$COP_R = \frac{\dot{Q}_L}{\dot{W}} = \frac{(h_1 - h_4)}{(h_2 - h_1)} \quad (11)$$

$$COP_{HP} = \frac{\dot{Q}_H}{\dot{W}} = \frac{(h_3 - h_2)}{(h_2 - h_1)} \quad (12)$$

It's important to note that a heat pump's COP changes depending on which way it's facing. The mathematical equation below describes the interaction between a heat pump and a refrigerator on the same cycle:

$$COP_{HP} - COP_R = 1 \quad (13)$$

For a Carnot cycle, the COP is given by the ratio of the absolute temperatures of the two sources.

$$COP_{Carnot} = \frac{T_H}{T_H - T_L} \quad (14)$$

Where:  $T_H$  is the absolute temperature of the high-temperature reservoir [K], and  $T_L$  is the absolute temperature of the low-temperature reservoir [K].



Due to practical limitations and energy losses, heat pumps cannot achieve the theoretical maximum efficiency of the Carnot cycle.

## **2.6. Subcooled and superheated refrigeration cycle**

In the simplest saturated refrigeration cycle, both the refrigerant vapor and liquid are assumed to be saturated before entering the compressor's suction and expansion valves, respectively. Saturated vapor can be further superheated by adding a superheating procedure before entering the compressor which will help to absorb more heat. Similarly, the subcooling procedure will cause a saturated liquid to get subcooled in front of the expansion valve allowing it to lose more heat.

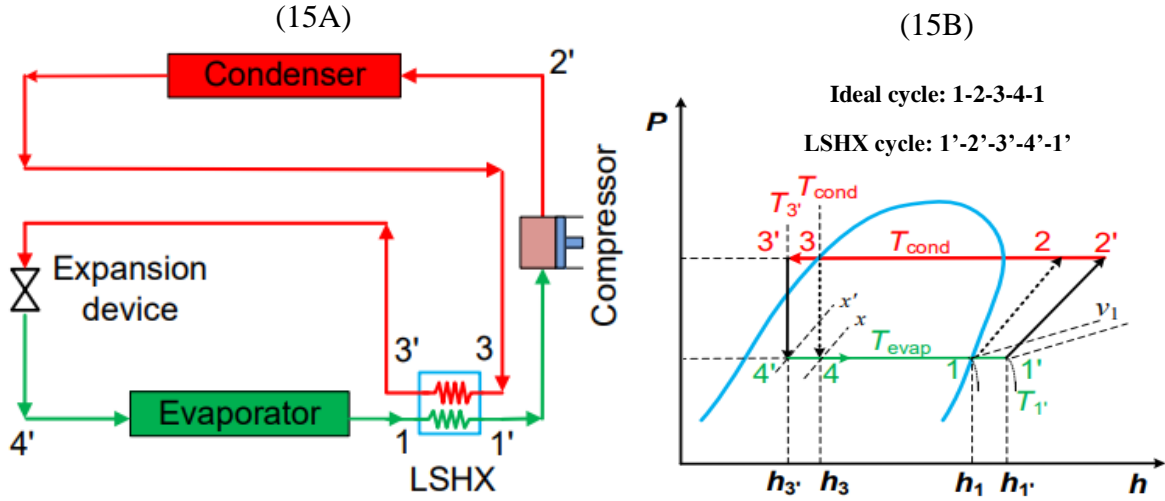
As will be seen in the following section, subcooling, and superheating are two of the methods for increasing the refrigeration cycle's efficiency [71]. They are typically used to improve performance (COP) and to avoid specific issues within the machines.

### **2.6.1. Subcooling**

By lowering the temperature of the liquid refrigerant as it leaves the condenser below its saturation point and guaranteeing that all amount of the refrigerant that reaches the expansion valve is in liquid form, the efficiency can be greatly increased. As a result of low vapor quality refrigerant entering the evaporator, the refrigerant absorbs more heat in the evaporator, which makes the COP increase, without increasing the input energy of the compressor [72]. Different reviewers classified the subcooling methods into different categories [73, 74], here are some of the most common:

#### Liquid-suction heat exchanger (LSHX)

The P-h diagram and schematic of a Liquid-suction heat exchanger (LSHX) air conditioning cycle are displayed in Figure 15. Assuming a saturated vapor phase at point 1 and a saturated liquid phase at point 3 in the basic cycle, using LSHX, we can transfer heat from the condenser's exit (the liquid line) to the compressor's inlet (the suction), when this happens, the saturated liquid transitions to the sub-cooled liquid state (point 3'), while the saturated vapor converts to the superheated vapor state (point 1'). The degrees of subcooling and superheating are respectively the temperature difference between points 3 and 3', and between points 1 and 1'. Consequently, the amount  $(h_1' - h_4')$  is bigger than  $(h_1 - h_4)$  which represents an increase in the cooling capacity [74].



**Figure 15.** Vapor compression refrigeration cycle with LSHX: (15A) A schematic sketch, (15B) The P-h diagram [74].

On top of that, it stops the liquid refrigerant from going into the compressor and the vapor from passing into the expansion mechanism. The increased superheating in the compressor suction is a drawback of employing LSHX since it raises the discharge temperature. Therefore, the superheating will increase the workload on the compressor. In other words, if cooling capacity rises thanks to LSHX, superheating rises right alongside it. Therefore, an increase in cooling capacity and compressor effort is directly proportional to the improvement in an air conditioner's performance. The COP will grow positively if the additional cooling capacity exceeds the additional work required by the compressor, and negatively otherwise.

#### Ambient subcooling

Vapor compression refrigeration systems with ambient subcooling use an additional heat exchange surface, which interacts with the ambient to subcool the liquid refrigerant. This method is used to downstream the condenser, increase the heat rejection to the ambient, and get higher COP.

Another method described in [75], is combining a separate heat exchanger (called the sub-cooler) and the condenser into one massive unit, under normal conditions, the sub-cooler in this setup is intended to reduce the temperature by  $8^{\circ}\text{C}$ . More heat transfer area is used since a lower condensing pressure allows for this. Therefore, the restriction on the expansion device must be increased to accomplish the targeted refrigerant subcooling.

### **2.6.2. Superheating**

There is a considerable chance that small particles of unvaporized liquid will be present in the vapor when the suction vapor is taken directly from the evaporator into the suction intake of the compressor without at least a minor amount of superheating. When wet vapor is sucked into the compressor's cylinder through wet suction, the compressor will not function properly and it might even break down, not to mention have its output energy lowered [72].

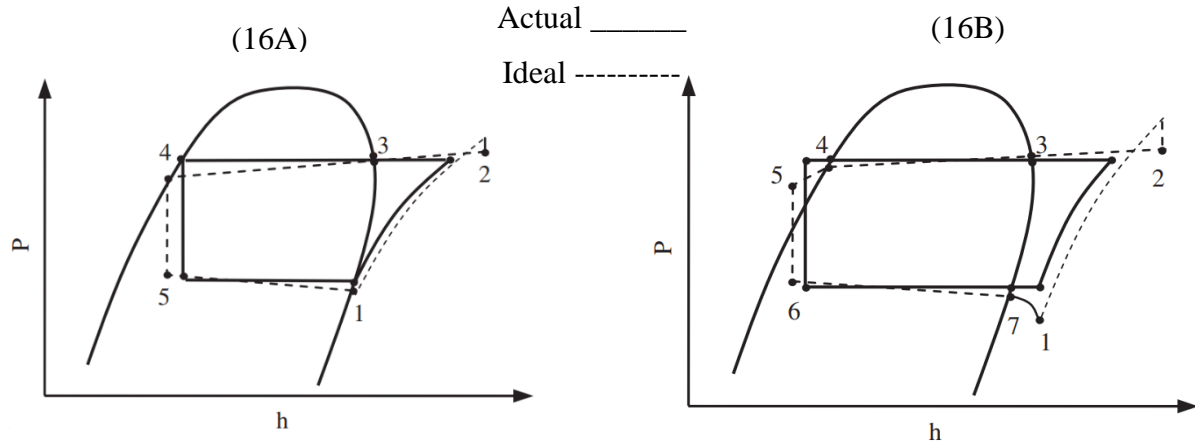
When compared to the saturated cycle, the superheated cycle has a larger refrigerating impact per unit mass of refrigerant. The COP for the superheated cycle is bigger than that of the saturated cycle because the rise in the refrigerating effect is proportionally more than the increase in the heat of compression.

Superheating can be found at the end of the evaporator, in the suction pipelines, or in the liquid-to-suction heat exchanger, either inside or outside the refrigerated area.

### **2.7. Real cycle**

Unlike the idealistic cycle shown in Figure 13, which assumes complete reversibility and no energy losses, the real cycle refers to the realistic thermodynamic processes that occur during the transformation and considers losses due to friction, heat transfer, pressure drops, temperature changes, and non-ideal behavior of the refrigerant [76]. These factors affect the system's performance and efficiency.

The understanding of thermodynamic processes and systems relies heavily on both the concept of reversibility and its opposite, irreversibility. When we refer to reversibility, we're talking about a mechanism through which the system and its environment can be reset to their original conditions. Entropy production and exergy dissipation are linked to irreversibility. An irreversible process is one in which neither the system nor its environment can be restored to its original conditions [77].



**Figure 16.** P-h diagrams of: (16A) typical refrigeration cycle, (16B) subcooled and superheated refrigeration cycle [72].

## 2.8. Simulation tools for refrigeration systems

Simulation tools offer the means to enhance the effectiveness, operation, and configuration of refrigeration cycles. Prior studies have explored the modeling capabilities of heat pumps, as exemplified by [78], who demonstrated the efficient modeling of energy characteristics in cooling circuits using straightforward software like Solkane 7.0. Additionally, alongside Solkane, one can also identify CoolPack and Coolselector 2 as three highly efficient technologies for overseeing and enhancing refrigeration systems.

### 2.8.1. CoolPack

CoolPack is a collection of simulation programs that can be used for designing, dimensioning, analyzing, and optimizing refrigeration systems developed by the Department of Mechanical Engineering, University of Denmark (DTU). It is a set of tools that can help with the study and design of refrigeration systems in many ways. The performance and efficiency of refrigeration cycles can be evaluated and improved with the help of CoolPack. CoolPack allows us to evaluate the efficiency and performance of the system in a variety of settings, thanks to its in-built capabilities for calculating component efficiencies and determining outlet statistics. CoolPack offers features such as property plots, thermodynamic and transport properties calculations, and a comparison of refrigerants. It allows for the assessment of the life cycle cost of refrigeration systems, considering factors such as installation, maintenance, and energy consumption.

### **2.8.2. Coolselector 2**

A modelization software offered by the Danish company Danfoss. Coolselector 2 helps maximize the effectiveness of heating, ventilation, air conditioning, and refrigeration systems by minimizing energy use. Select the best parts for the design after running quantitative calculations based on the operating conditions, which include parameters like cooling capacity, temperature, and pressure.

### **2.8.3. Solkane**

The Solkane program is a powerful calculation tool designed to analyze thermophysical properties and perform various calculations related to refrigeration systems. It offers several features and modules that enable customization and calculation of different parameters. Users can adjust table settings, calculate single points, and examine many refrigerant cycles inside the same software. Detailed graphics are also included to help readers better understand the findings.

### **3. Materials and methods**

In this work, I embark on an energetic investigation and comprehensive performance analysis of a solar-assisted heat pump, aimed at advancing sustainable heating applications. Leveraging a wealth of data collected throughout several days, including solar radiation, temperatures at critical points, compressor pressures, and power consumption. Through meticulous analysis and a rigorous energy balance equation, we unveil crucial insights into energy transfer efficiency, enthalpy changes, and overall system performance. Additionally, we consider the impact of ambient conditions on the system and more precisely the condenser's behavior, allowing us to assess its adaptability to various environmental factors. By identifying potential areas for optimization, this thesis seeks to contribute to the development of energy-efficient and eco-friendly heating technologies. The findings presented herein offer a robust foundation for enhancing solar-assisted heat pump designs and encouraging a sustainable transition toward a greener future.

#### **3.1. Materials and equipment**

The experiment took place at the energetic building's laboratory of the Hungarian University of Agriculture and Life Sciences, spanning four distinct days in the month of July (14th, 17th, 24th, and 28th). The experimental setup consists of two primary components: an external flat plate solar collector positioned on the rooftop of the aforementioned building and an internal heat pump situated within the laboratory itself. The integration of these components occurs at the evaporator level, facilitating the exchange of heat between the antifreeze flowing through the flat plate solar collector and the refrigerant circulating in the heat pump. This interaction enables the efficient transfer of thermal energy between the two blocks. For a visual representation, refer to the schematic Fig.17 provided below, outlining the experimental configuration.

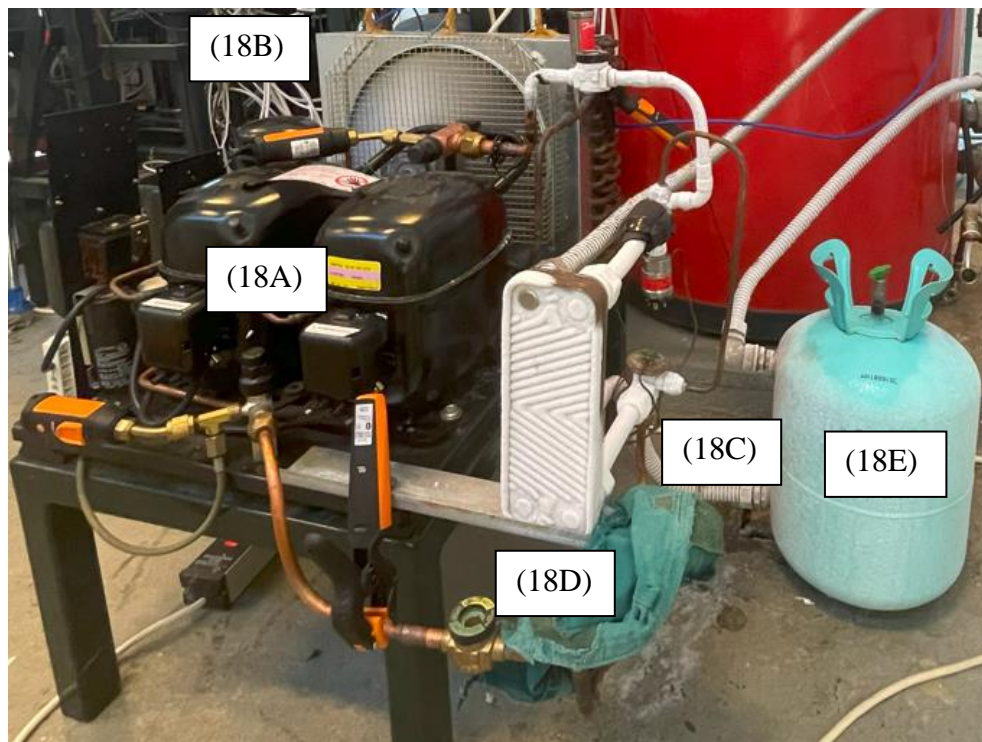


of 70% water and 30% antifreeze was circulated through a network of tubes positioned within the collector. As sunlight struck the surface of the collector and got absorbed, it facilitated the heating of the antifreeze fluid circulating within the tubes. By this means, solar energy was effectively converted into heat energy.

Various parameters were measured in this block; the fluid temperature at both inlet and outlet of the solar collector, and crucial environmental factors such as solar radiation and ambient temperature were meticulously recorded to understand their impact on the overall system performance.

### 3.1.2. Heat Pump

In the depicted second component, as is shown in Figure 18, which corresponds to the heat pump, a condensing unit equipped with a twin compressor manufactured by the renowned company Danfoss, was employed.



**Figure 18.** The heat pump, (18A): Twin compressor, (18B): The condenser, (18C): The expansion valve, (18D): The evaporator (18E): The tank.



### Compressor

Danfoss SC18/18CL-BP compressor (Figure 18A), was employed in this study. This twin-compressor model offers high efficiency, reliability, and low noise levels. The inlet and outlet temperatures and pressures of the refrigerant, as well as the instantaneous electricity consumption of the compressor, were measured during the experiment.

### Condenser

In this experiment, an axial fan condenser was used (Figure 18B), spinning at a velocity of 1300 RPM. The dimension of the condenser is  $(384 \times 324 \times 100)$  mm and includes 4 rows of tubes. The fan has a maximum airflow rate of 160 cubic meters per hour, can run on 230 volts AC, and consumes around 14 watts of power. The fan was designed to function between 30 and 60 degrees Celsius.

### Expansion valve

A mechanical expansion valve suitable for use with R404a, R22, and R407c was employed (Figure 18C). The pressure drop caused by the valve was close to 8 bar, and the maximum refrigeration power of the valve was 3 kW, the expansion valve is placed before the evaporator and after the condenser.

### Heat exchanger-Evaporator

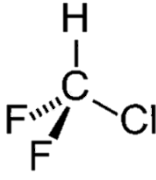
The evaporator utilized in the present study was a CBH 16-9H SWEP-sized plate heat exchanger placed on a horizontal mount (Figure 18D) and had a capacity of 35 kW. The high-quality stainless steel plates used in the heat exchanger's compact, brazed plate design made it both long-lasting and corrosion-proof. In this test, the CBH 16-9H heat exchanger has an overall heat transfer coefficient of  $4500 \text{ W/m}^2 \cdot \text{K}$ .

#### **3.1.3. Refrigerant**

Our heat pump operated using R22, which shares similarities with ammonia as a medium-pressure refrigerant. R22 is a nonflammable and safe refrigerant from a toxicological perspective. It has remained a favored option for an extended period owing to its advantageous thermodynamic

characteristics, making it efficient in heat transfer and cooling applications. Some of its notable properties are listed in Table 4 below, sourced from the Solkane software.

**Table 4.** Properties of R22 refrigerant

<b>Composition by mass</b>	Carbon (C): 40.9% + Hydrogen (H): 4.5% + Chlorine (Cl): 35.6% + Fluorine (F): 18.9%
<b>Formula</b>	Chlorodifluoromethane (CHClF <sub>2</sub> ) 
<b>Molecular weight</b>	86.5 kg/kmol
<b>Freezing point</b>	-160.6°C
<b>Boiling point</b>	1.013 bar / -40.8°C
<b>Evaporating temperature range</b>	[-40°C , +5°C]
<b>Critical temperature</b>	96.15°C
<b>Critical Pressure</b>	49.0 bar
<b>EC standard limit value</b>	1,000 vol.-ppm
<b>ODP value</b>	94.5%

#### 3.1.4. Storage tank

The storage tank used in this experiment is a vertical cylindrical container made of steel (Figure 18E), specifically designed to hold a capacity of 13 liters. Its primary purpose is to serve as a reservoir for storing the heated antifreeze, which has absorbed thermal energy from the flat plate solar collector. This tank is strategically connected to both the outlet of the flat plate solar collector and the heat exchanger.

#### 3.2. Data collection

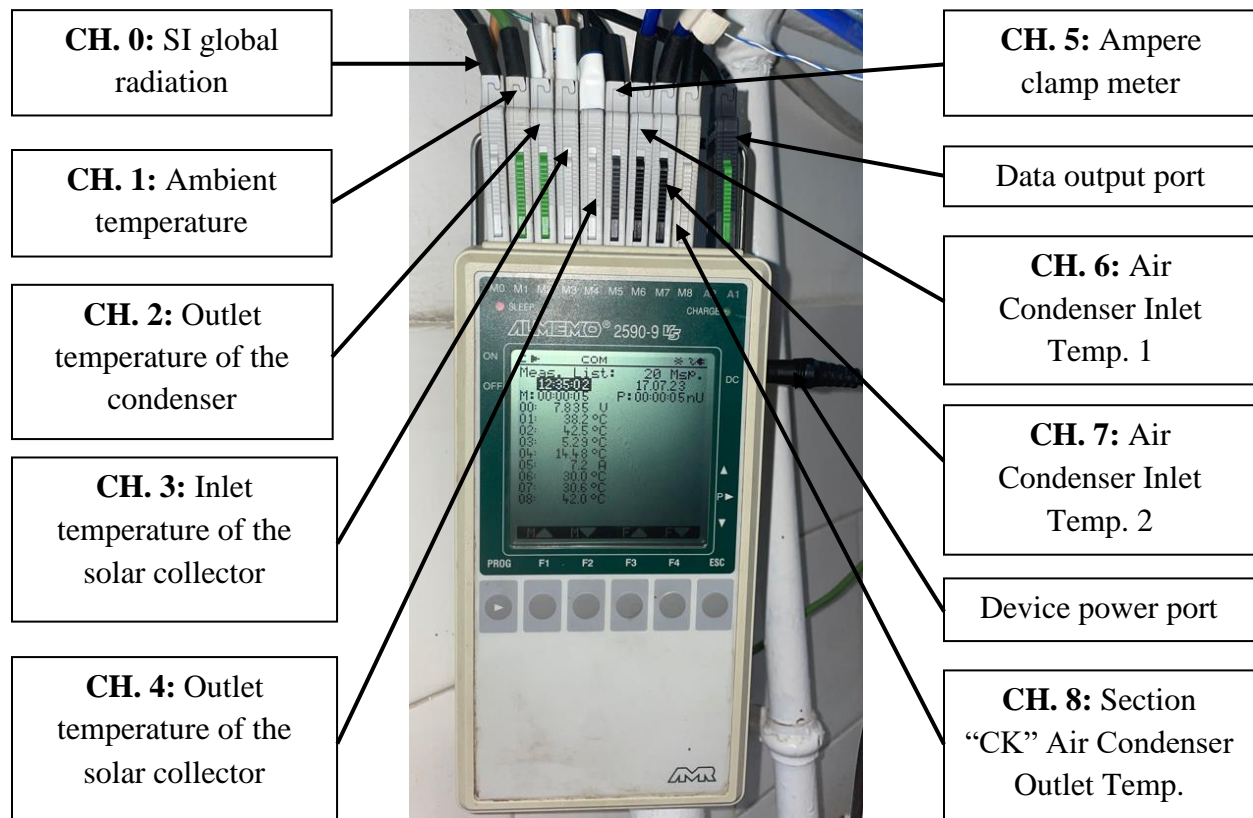
In our experiments, a comprehensive range of parameters was measured to ensure accurate and thorough analysis. Among the parameters collected were the global radiation, the temperature readings at different points within the system, and the pressure of the compressor.

To carry out these precise measurements, we employed a variety of advanced and reliable instruments, each tailored to the specific parameter being assessed.

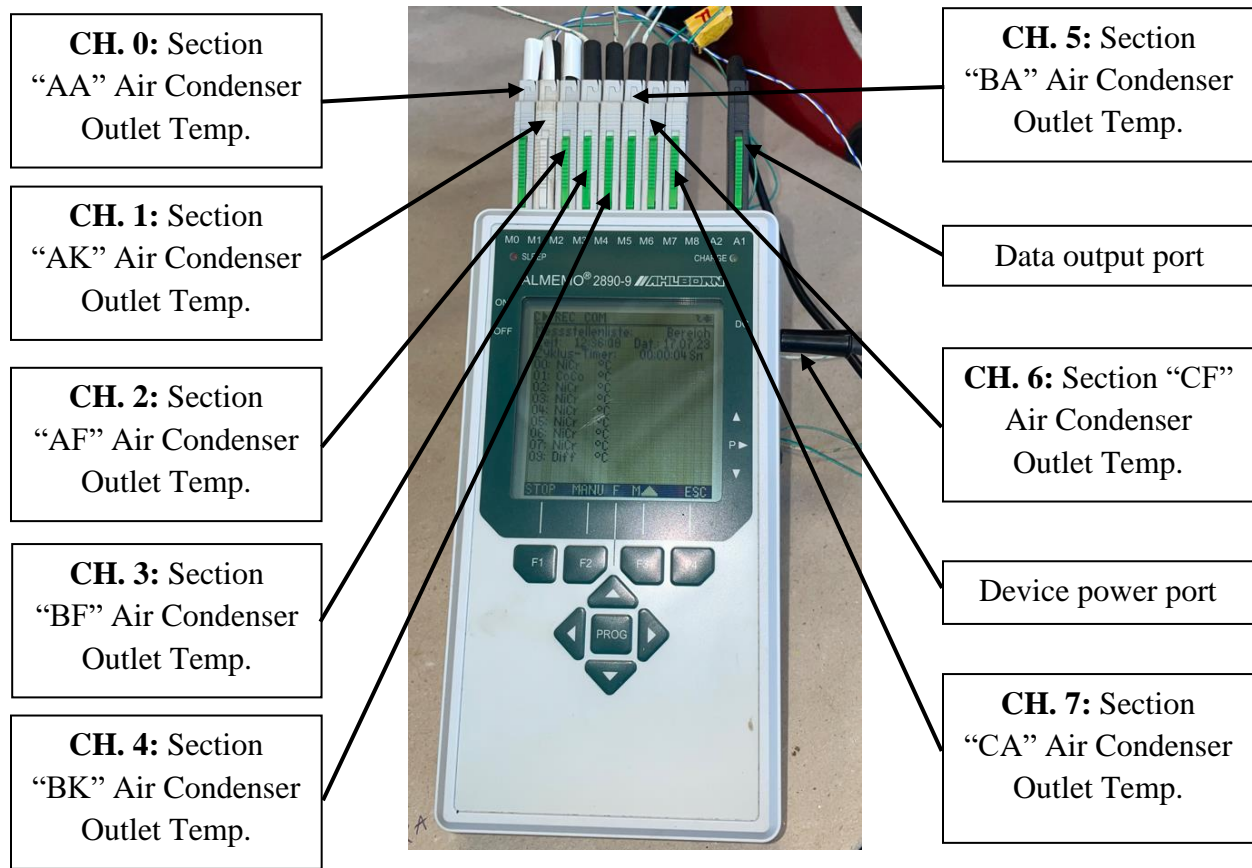
### 3.2.1. ALMEMO system

The ALMEMO system is an advanced and versatile data acquisition and measurement solution designed for precision and flexibility across various scientific and industrial applications, developed by Ahlborn Mess-und Regelungstechnik GmbH (AHLBORN). The ALMEMO system consists of a range of data loggers, sensors, and modules that are seamlessly integrated to establish a full ecosystem for data collecting.

Two ALMEMO devices with the same type have been used to collect the temperatures, solar irradiation, and the current intensity of the system, each of them has eight channels where each channel (CH.) displays the value of what the sensor has measured (Fig. 19 + Fig. 20).



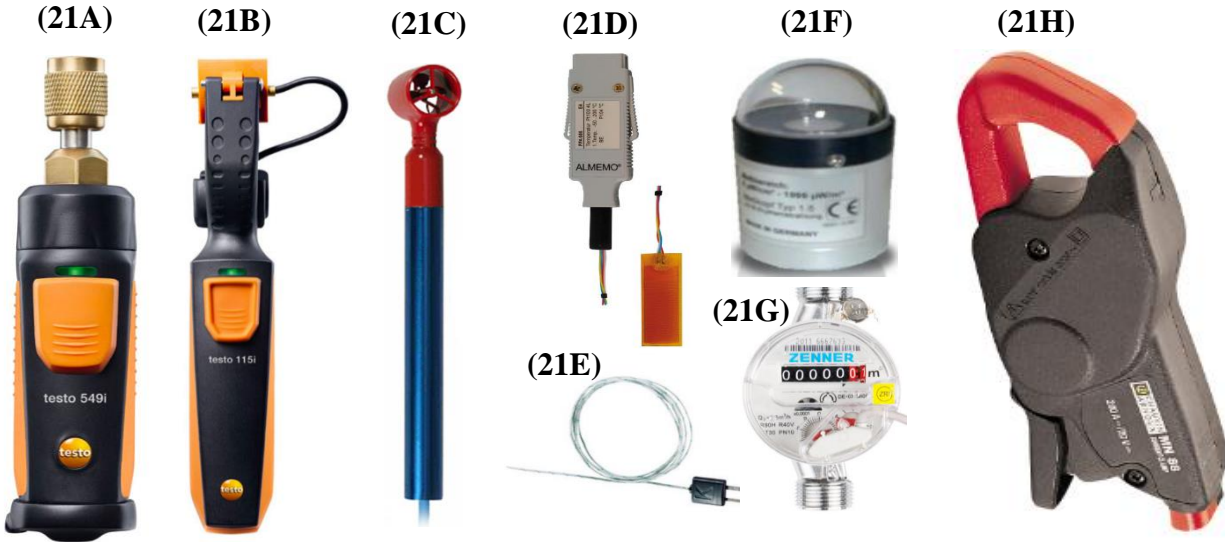
**Figure 19.** 1<sup>st</sup> ALMEMO device (Model 2590-9).



**Figure 20.** 2<sup>nd</sup> ALMEMO device (Model 2890-9).

### 3.2.2. Measuring equipment

In our experimental arrangement, we strategically positioned multiple sensors and devices to gather essential data and monitor the system’s performance. The comprehensive collection of these instruments is presented in Figure 21, while each specific device is described in detail below.



**Figure 21.** Measuring instruments and sensors, (21A): Testo 549i Bluetooth high-pressure gauge, (21B): Testo 115i Bluetooth clamp thermometer, (21C): Micro rotating vane anemometer, (21D): Temperature sensor “Pt 100”-Type, (21E): Temperature sensor “K”-Type, (21F): Si global radiation sensor, (21G): Water meter gauge, (21H): Amper clamp meter.

#### Testo Smart Probes 549i

We used two sets of Testo Smart Probe 549i to measure the pressure and temperature at both the input and output of the compressor. Each set of Testo Smart Probe 549i consisted of two devices: the Testo 549i Bluetooth high-pressure gauge (Figure 21A) and the Testo 115i Bluetooth clamp Thermometer (Figure 21B). To gather the data efficiently, we connected all four devices to the Testo Smart Probes application on a smartphone using Bluetooth. The measurements were recorded every second with high precision, offering a resolution of 0.1°C for temperature and 0.01 bar for pressure.

#### Airflow

The use of a third ALMEMO (MODEL 2890-9) device including a micro rotating vane Anemometer (Figure 21C) enhances the precision and accuracy of air velocity measurements. This innovative instrument is widely recognized for its ability to determine air velocity with a high level of precision. The device’s intricate design enables precise assessments of airflow speed and direction in various situations. We utilized this device to ascertain the airflow at the condenser level (inlet and outlet).

#### Temperature sensors

We incorporated two types of temperature sensors in this experiment. The first type is the “Pt 100”-Type sensor (model number 13070020, manufactured by ALMEMO FP A611-S01 Norm E4), known for its high accuracy and stability in measuring temperature (Fig. 21D). It has an operating range of  $-10$  to  $110\text{ }^{\circ}\text{C}$ . The accuracy of this sensor was  $\pm 0,1\text{ }^{\circ}\text{C}$ , and the resolution was  $0,01\text{ }^{\circ}\text{C}$ . To achieve consistent temperature data, the sensor was positioned at both the inlet and outlet of the solar collector.

The second type is the “K”-type sensor (Figure 21E), which is also widely used for its reliability in temperature measurements, especially in high-temperature environments. The K-type thermocouple had an operating range of  $-10$  to  $+110\text{ }^{\circ}\text{C}$  and a rated accuracy of  $\pm 0,1\text{ }^{\circ}\text{C}$ . The sensors of this kind were strategically positioned at various locations throughout the system to capture the necessary data, including the ambient temperature and the temperature of the refrigerant subsequent to condensation, two sensors were strategically placed on the front surface of the condenser, labeled as “1” and “2” to measure the temperatures of the air entering the condenser. Conversely, nine sensors were affixed to the backside of the condenser, designated as “AF”, “BF”, “CF”, “AK”, “BK”, “CK”, “AA”, “BA” and “CA” for air outlet temperatures.

#### Si global radiation sensor

A Si global radiation sensor equipped with a silicon photodiode was used to measure the intensity of solar radiation per day (Figure 21F), and the data was collected by the ALMEMO system, for detailed characteristics of this device, see Annex A.

#### Water meter

The flow meter used in this experiment is a single-jet dry dial cold water meter (model ETKD-N), it is well-suited for general metering tasks in domestic, small commercial, and industrial settings, especially when there is a requirement to measure extremely low flow rates accurately (Figure 21G). The flow meter was installed in a vertical orientation. Based on the measurements obtained, the volume flow of antifreeze entering the solar collector was recorded at 180 liters per hour.

#### Ampere clamp meter

The amount of current consumed by the compressor was determined by linking up an ampere clamp meter (Model MN88) to its power supply (Figure 21H). The amperage clamp meter measured from 1 to 150 A with a  $0,1\text{ [A]}$  resolution. This device can clip any cable up to 20 mm in diameter in installations, making it useful for measurements even in inaccessible areas. The ALMEMO system stored the amperage clamp meter readings taken during the experiment.

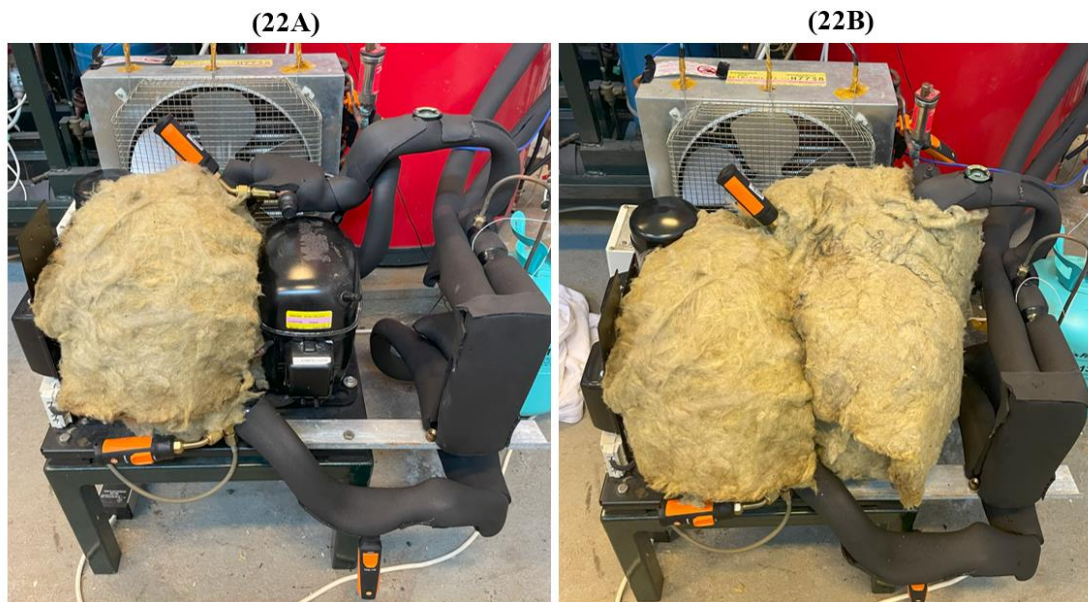
### 3.3. Control system

During the course of this experiment, the inlet temperature entering the solar collector was left unregulated. The sole parameter under indirect control was the power consumption of the compressor. Throughout the study, we conducted measurements using two compressors in one set of tests and a single compressor in the remaining two tests on the left side.

### 3.4. Description of the experiment

#### 3.4.1. System insulation strategy

In this trial, we have employed an inorganic fibrous material as insulation for the compressor(s) of the heat pump, capitalizing on its exceptional thermal properties, and non-combustible nature. One of the compressors was covered with this insulation material, while in another case; we insulated both compressors to thoroughly evaluate losses compared with the non-insulated scenario. In addition to utilizing the inorganic fibrous material for compressor insulation, we extended the application to cover the tubes of the heat pump and those connected to the solar collector (inlet and outlet tubes) with rubber insulation. This choice of insulation was deliberate, as class rubber insulation boasts exceptional thermal properties, making it an ideal option for ensuring optimal heat transfer and retention within the entire system. Figure 22 below shows how the insulation was placed within the system.





**Figure 22.** The insulated system: (22A): Partially insulated system, (22B): Totally insulated system.

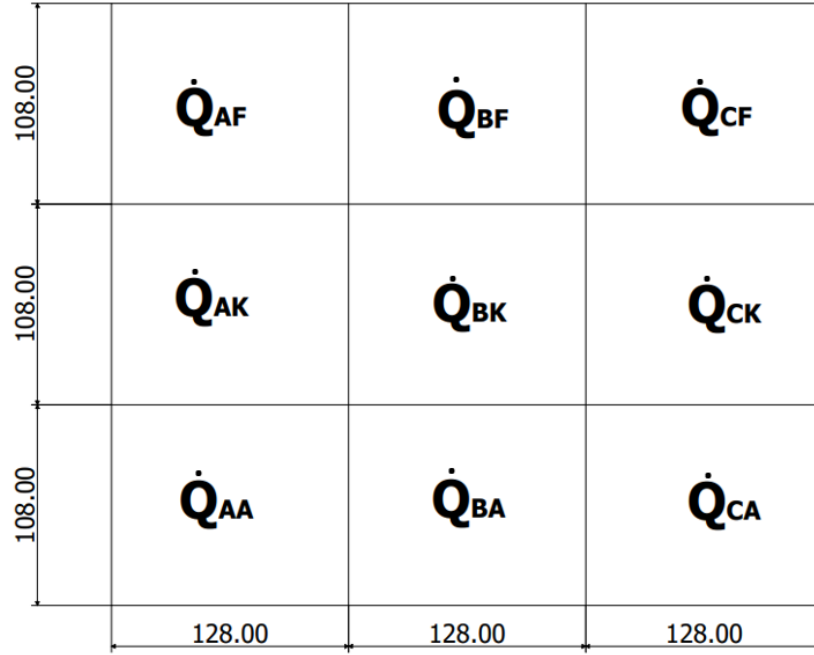
The primary objective of insulating the setup was to minimize heat losses during the operation, thereby significantly enhancing the overall efficiency of the system. This proactive insulation approach not only reduces energy wastage but also contributes to lowering operational costs, making the entire system more sustainable and effective. The trials were conducted across a span of four days, for each day different setup was tabulated as follows:

**Table 5.** Experiment schedule and explanation

Day	Date	Description	Figure
1 <sup>st</sup> day	July 14, 2023	One compressor running without insulation.	18
2 <sup>nd</sup> day	July 17, 2023	Two compressors running without insulation.	18
3 <sup>rd</sup> day	July 24, 2023	One compressor running with partial insulation (Insulation at the level of one compressor and the tubes).	22A
4 <sup>th</sup> day	July 28, 2023	Two compressors running with total insulation (Insulation at the level of two compressors and the tubes).	22B

To accurately measure the system's released heat, we arranged nine sensors symmetrically at the condenser's output and added two sensors at its inlet. Data from these sensors was collected using both ALMEMO devices (as depicted in Figures 19 and 20). The drawing in Figure 23 demonstrates the division of the condenser's back surface, with each sensor centrally positioned within its section. This setup enabled us to measure the difference of the air temperature flowing at the level of the condenser, and subsequently, the heat emitted per section. We then summed the heat from each section and applied Equation (16), detailed below, to determine the condenser's total heat discharge.





**Figure 23.** Condenser surface partitioning.

### 3.4.2. Adopted calculations

Energy balance equation for the system:

$$\dot{Q}_H = \dot{Q}_S + P_{eff} + E_{loss} \quad (15)$$

Where:

$\dot{Q}_H$ : The total energy released by the condenser [W], can be calculated as follows:

$$\dot{Q}_H = \sum_{i=AF}^{CA} \dot{Q}_i = \dot{Q}_{AF} + \dot{Q}_{BF} + \dot{Q}_{CF} + \dot{Q}_{AK} + \dot{Q}_{BK} + \dot{Q}_{CK} + \dot{Q}_{AA} + \dot{Q}_{BA} + \dot{Q}_{CA} \quad (16)$$

The energy released by the condenser per section ( $\dot{Q}_i$ ) could be determined as follows:

$$\dot{Q}_i = \dot{m}_{air} \cdot c_{air} \cdot (T_i - T_{Inlet}) \quad (17)$$

With:

$\dot{m}_{air}$ : The mass flow of the air at the level of the condenser [Kg/s].

$c_{air}$ : The specific heat capacity of the air [J/kg.°C].

$T_i$ : The average outlet air temperature of the specific section of the condenser [°C].

$T_{Inlet}$ : The inlet air temperature of the condenser [°C].

$\dot{Q}_S$ : The obtained heat from the solar collector [W] can be calculated as follows:

$$\dot{Q}_S = \dot{m}_{Antifreeze} \cdot c_{Antifreeze} \cdot (T_{Outlet} - T_{Inlet}) \quad (18)$$

With:

$\dot{m}_{Antifreeze}$ : The mass flow of the Antifreeze at the level of the condenser [Kg/s].

$c_{Antifreeze}$ : The specific heat capacity of the antifreeze [J/kg.°C].

$T_i$ : The outlet temperature of the solar collector [°C].

$T_{Inlet}$ : The inlet of the solar collector [°C].

$\dot{Q}_S$ : The obtained heat from the solar collector [W] can be calculated as follows:

$P_{eff}$ : The power consumed by the compressor [W], can be calculated using the following formula:

$$P_{eff} = U_{eff} \cdot I_{eff} \quad (19)$$

Where:

$U_{eff}$ : The voltage from the grid, is equal to 230 [V].

$I_{eff}$ : The consumed current by the compressor(s) [A].

$E_{loss}$ : Energy loss of the system [W], can be concluded from the equation (15) as follows:

$$E_{loss} = \dot{Q}_H - \dot{Q}_S - P_{eff} \quad (20)$$

#### 4. Results and discussion

The data collected throughout the day was primarily obtained from two separate computers that gathered information sent by the two ALMEMO devices. Additionally, a smartphone was utilized to record data from the Testo instruments. To ensure a reliable evaluation, I focused on collecting data during the overlapping time intervals with a time difference of  $\pm 1s$  between the two ALMEMO devices, considering that data was provided every 5 s. Subsequently, I retrieved data from the Testo probes within the range specified by the ALMEMO devices, as the Testo recorded

data every second. All the data assessed each day is confined to the shared timeframe from 10:30 AM to 2:30 PM. This particular time range was selected due to preceding and subsequent transient conditions, strong weather variations, and occasional instances of data loss, as detailed in Table 6 below.

**Table 6.** Evaluation time frames.

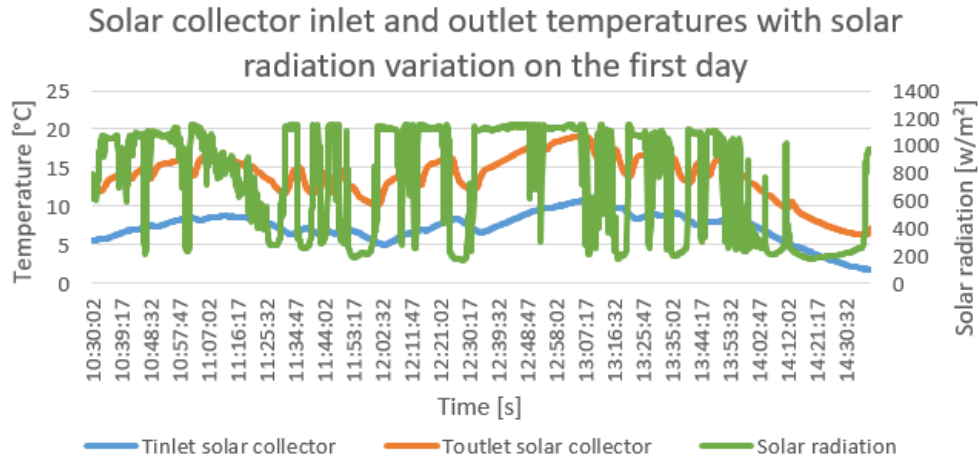
Day No.	Data loss period [Time]	No. of operating compressors	System insulated?	Evaluation period [Time]
1 <sup>st</sup>	[9:00-10:30]	1	No	[10:30-14:30]
2 <sup>nd</sup>	[14:30-15:00]	2	No	[10:30-14:30]
3 <sup>rd</sup>	No data loss	1	Yes	[10:30-14:30]
4 <sup>th</sup>	No data loss	2	Yes	[10:30-14:30]

#### **4.1. Solar collector integration and ambient conditions affect**

The operational performance of our experimental setup, including both the inlet and outlet of the solar collector, is profoundly influenced by the surrounding environmental conditions, mainly the solar radiation intensity and ambient temperature. Each day's outcomes at both the inlet and outlet points are meticulously presented, thereby facilitating an in-depth comprehension of the profound influence that the integration of solar collectors exerts on the operational dynamics of the heat pump. Furthermore, this analysis serves as a pivotal step in unraveling the intricate energy-related inquiries we aim to address.

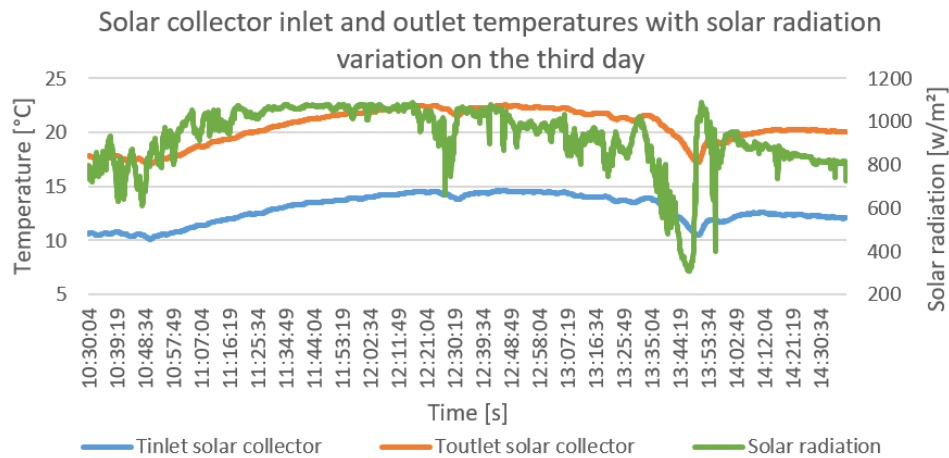
##### **4.1.1. For a single compressor scenario (the first and the third day)**

Below, you will find the measured environmental data for both scenarios where only a single compressor was operational, besides the temperature inlet and outlet of the solar collector. This data sheds light on notable contrasts between the two cases. On the day when the system lacked insulation (the solar radiation level was relatively low, approximately  $741 [W/m^2]$  on average). This lower solar input coincided with a more modest variation in the temperature of the glycol mixture, registering a change of only  $6,72 ^\circ C$ . The temperature fluctuations directly mirror the variations in solar radiation intensity, as evident in the visual representation provided in Figures 24 and 25 below.



**Figure 24.** Impact of solar radiation on the outlet temperature of the solar collector on the first day (14 July).

In contrast (Figure 25), the insulated system exhibited a contrasting pattern, the average solar radiation intensity was recorded as  $932 \text{ W/m}^2$ . Alongside this heightened solar exposure, the variation in glycol mixture temperature expanded to  $7,58^\circ\text{C}$ .



**Figure 25.** Impact of solar radiation on the outlet temperature of the solar collector on the third day (24 July).

The graphical representations provide a clear visual depiction of how ambient conditions exert a significant influence on outlet temperature outcomes. This influence remains constant irrespective of the presence of insulation. To consolidate the information from the graphs, we have succinctly summarized the pertinent data in the following tables, 7 and 8.

**Table 7.** First day: Average measured and calculated data of the solar collector and ambient conditions.

<b>Data</b>	<b>Solar radiation [W/m<sup>2</sup>]</b>	<b>Ambient temp. [°C]</b>	<b>Inlet temp. [°C]</b>	<b>Outlet temp. [°C]</b>	<b><math>T_{out} - T_{in}</math> [°C]</b>
<b>Avg.</b>	741,16	29,22	7,50	14,22	6,72

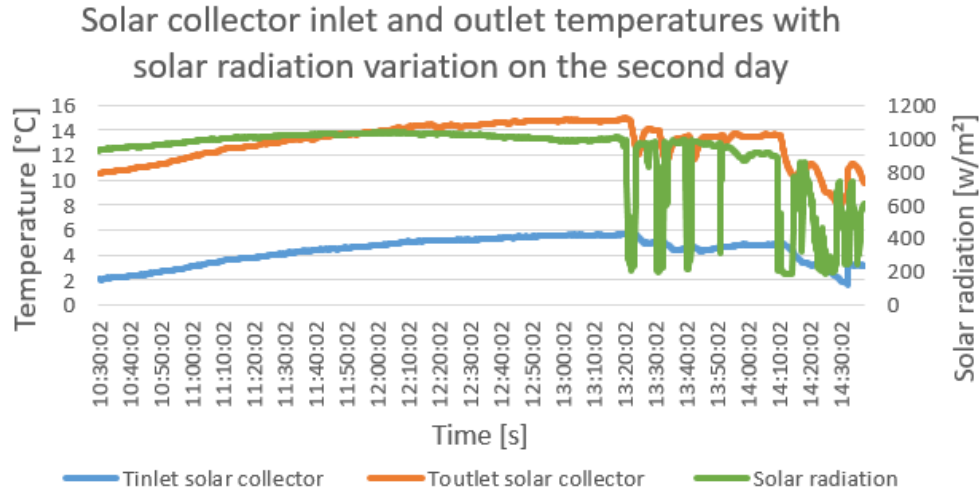
**Table 8.** Third day average measured and calculated data of the solar collector and ambient conditions.

<b>Data</b>	<b>Solar radiation [W/m<sup>2</sup>]</b>	<b>Ambient temp. [°C]</b>	<b>Inlet temp. [°C]</b>	<b>Outlet temp. [°C]</b>	<b><math>T_{out} - T_{in}</math> [°C]</b>
<b>Avg.</b>	932,32	33,23	12,92	20,50	7,58

On the second day, the average ambient temperature exceeded that of the first day by 4 °C. However, it is noteworthy that we observed only a marginal temperature variation of less than one degree (if we compare  $\Delta T$  ( $T_{out} - T_{in}$ ) in both previous tables). Consequently, this phenomenon has implications for the reduction of heat absorption from the solar collector ( $\dot{Q}_S$ ), as it is intricately linked to the temperature difference (the volume flow of the antifreeze remained constant).

#### **4.1.2. In a dual-compressor scenario (the second and the fourth day)**

The graphs presented in Figures 26 and 27 illustrate the fluctuations in measured parameters under two distinct conditions: with and without insulation. These graphs reveal a clear relationship between solar radiation and mixture temperature.



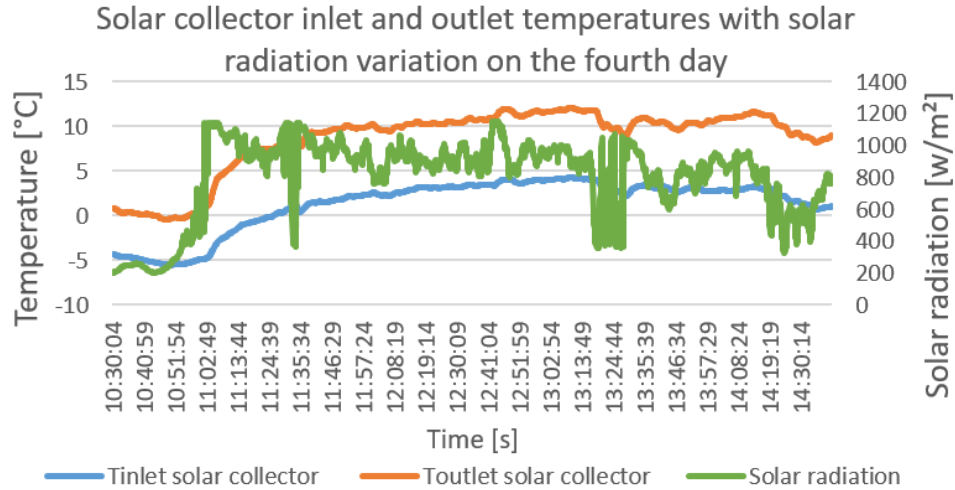
**Figure 26.** Impact of solar radiation on the outlet temperature of the solar collector on the second day (17 July).

On the second day, when insulation was not used, we observed an average ambient temperature of 37 °C, additionally, the average solar radiation stood at 920 [ $W/m^2$ ], as detailed in Table 9, indicating warm conditions during the data collection.

**Table 9.** Second day: Average measured and calculated data of the solar collector and ambient conditions.

Data	Solar radiation [ $W/m^2$ ]	Ambient temp. [°C]	Inlet temp. [°C]	Outlet temp. [°C]	$T_{out} - T_{in}$ [°C]
Avg.	919,74	36,60	4,39	13,12	8,73

On the other hand, when the system was insulated, we found the same changes with variation of the values, Figure 27 shows this variation during the day and they are summarized in Table 10 below.



**Figure 27.** Impact of solar radiation on the outlet temperature of the solar collector on the fourth day (28 July).

On this particular day, the recorded average solar radiation measured at 805,69 [ $W/m^2$ ]. This value marked a notable decrease compared to the previous day when solar radiation levels were considerably higher. Additionally, the ambient temperature on this day was notably lower, 27,30 °C, registering a temperature that was 9 °C lower than on the preceding day.

**Table 10.** Fourth day: Average measured and calculated data of the solar collector and ambient conditions.

Data	Solar radiation [ $W/m^2$ ]	Ambient temp. [°C]	Inlet temp. [°C]	Outlet temp. [°C]	$T_{out} - T_{in}$ [°C]
Avg.	805,69	27,30	1,34	8,56	7,22

Despite the reduced solar radiation and lower ambient temperatures, the system's outlet temperature remained relatively stable (only a difference of 1,51 °C was found). This intriguing phenomenon suggests that the solar panel system's efficiency was able to harness and utilize solar energy effectively, even under less favorable environmental conditions. This resilience to fluctuating external factors highlights the potential for optimizing solar energy utilization within such a system, irrespective of the prevailing ambient conditions.

In order to conduct a fair and thorough comparison of insulated and uninsulated designs, it is important to recognize that environmental factors can make it difficult to determine the impact of

insulation. This is due to the fact that on a particular day, we encountered conditions that were more conducive to the evaluation of the insulation's effectiveness compared to its direct influence on the system's output.

#### 4.2. Compressor(s) performance analysis

The tables 11, 12, 13, and 14 below showcase the compressor's input and output parameters as recorded by the Testo's instruments. The key data under evaluation include temperatures, pressures, and the average power consumption of the machine.

##### 4.2.1. For a single compressor scenario (the first and the third day)

Specifically, Table 11 displays values for non-insulated conditions (1<sup>st</sup> day), while Table 12 displays values for insulated conditions (3<sup>rd</sup> day) of the aforementioned parameters. For a detailed insight into the day-long fluctuations of these parameters, refer to the graphs in Annex B.

In this part, number "1" corresponds to the input data, while number "2" pertains to the output one.

**Table 11.** First day: Average measured and calculated data of one compressor: Non-insulated HP.

Data	T <sub>1</sub> [°C]	T <sub>2</sub> [°C]	$\Delta T$ [°C]	P <sub>1</sub> [bar]	P <sub>2</sub> [bar]	$\varepsilon P = P_2/P_1$	P <sub>eff</sub> [W]
Avg.	33	76,04	43,04	3,4	14,66	4,31	897,31

**Table 12.** Third day: Average measured and calculated data of one compressor: Insulated HP.

Data	T <sub>1</sub> [°C]	T <sub>2</sub> [°C]	$\Delta T$ [°C]	P <sub>1</sub> [bar]	P <sub>2</sub> [bar]	$\varepsilon P = P_2/P_1$	P <sub>eff</sub> [W]
Avg.	37,85	73,16	35,31	3,90	15,93	4,08	949,11

In the non-insulated heat pump system, we noted a more significant temperature differential at the compressor's output, with a recorded difference of 7,73°C higher than the insulated system. This disparity can be attributed primarily to the ambient conditions which is the ambient temperature (since the heat pump is inside the building where the solar radiation cannot reach it). On the day of insulation, the ambient temperature was higher, but the insulated system couldn't fully capitalize on this advantage, as was the case on the first day of measurement, following the pressure as well due to the refrigerant properties.



In addition, it is notable that the compressor in the insulated configuration consumes more energy (with a relatively small value of about  $\Delta P_{eff} = 52 \text{ W}$ ), which indicates that the compressor needs to work more efficiently in the insulated setup to maintain the target temperature due to the reduced amount of heat exchange with the surroundings, especially at the level of the evaporator, where it was exchanging the heat only from the antifreeze rather than use double source mentioning the environment as the second one. Simultaneously, suboptimal insulation can exacerbate this energy demand by allowing undesirable heat transfer, undermining system efficiency. Therefore, to enhance the performance of the insulated setup, careful attention must be paid to both insulation quality and the compressor's workload management.

#### 4.2.2. In a dual-compressor scenario (the second and the fourth day)

In a careful review of the data presented in Tables 13 and 14, we can observe that the differences in compressor output pressure are marginal within this specific system. Yet, when it comes to temperature variations, a stark contrast becomes apparent. The non-insulated setup displays a temperature that is higher by  $13^\circ\text{C}$  compared to its insulated counterpart. This trend remains consistent even when only a single compressor is operational and for the same reasons that early mentioned. Day-long variations of these parameters are illustrated in the graphs in Annex B.

**Table 13.** Second day: Average measured and calculated parameters of two compressors: Non-insulated HP.

Data	$T_1$ [°C]	$T_2$ [°C]	$\Delta T$ [°C]	$P_1$ [bar]	$P_2$ [bar]	$\varepsilon P = P_2/P_1$	$P_{eff}$ [W]
Avg.	39,23	88,17	48,94	2,60	17,69	6,80	1632,29

**Table 14.** Fourth day: Average measured and calculated parameters of two compressors: Insulated HP.

Data	$T_1$ [°C]	$T_2$ [°C]	$\Delta T$ [°C]	$P_1$ [bar]	$P_2$ [bar]	$\varepsilon P = P_2/P_1$	$P_{eff}$ [W]
Avg.	40,91	76,47	35,56	2,50	16,37	6,55	1500,48

When analyzing the average power consumption of the compressors  $P_{eff}$ , a clear distinction emerges: when the compressors are insulated, they consume significantly lower energy compared to their uninsulated counterpart, this discrepancy in power usage amounts to substantial energy savings of nearly 132 W. Interestingly, this observation was less pronounced when only a single compressor was in operation. However, as the number of operating compressors increases, the benefits of insulation become increasingly clear. This suggests that the insulation plays a crucial role in enhancing the efficiency of the compressors, especially when multiple units are running concurrently.

The underlying reason might be that as the number of compressors increases, the collective heat generation and associated thermal losses escalate, making the role of insulation even more pivotal in maintaining operational efficiency and thermal stability. In this light, the concept of thermodynamic reversibility becomes particularly relevant. A process is deemed reversible if it can revert to its initial state without any net change in the surrounding environment. In the case of these compressors, insulation helps moving the system closer to this idealized reversible state by minimizing energy losses due to external thermal factors. This correlation between insulation and reversibility underscores the importance of minimizing energy loss, both for the sake of efficiency and for the broader goal of creating systems that operate in harmony with their environments.

### **4.3. Heat pump efficiency**

In this evaluative section, a meticulous analysis of the Coefficient of Performance (COP) of the heat pump is undertaken. Two facets of the COP are under scrutiny:

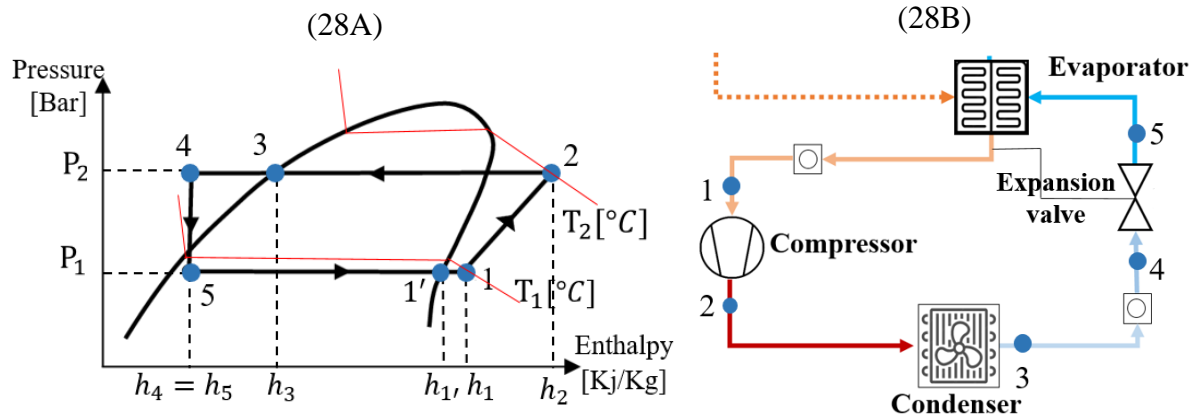
- First, there's the theoretical COP. This value is gleaned from simulations based on the refrigeration cycle, carried out with the aid of the CoolPack software. It provides an idealized perspective of the heat pump's performance, offering a benchmark against which real performance can be compared.
- At the same time, we assess the actual or real COP. This is determined empirically from experimental data, by taking the ratio of the average heat released by the condenser to the average effective power consumed by the compressor.

My analysis delves deeper into the thermodynamics of the system. I've explored the entropy changes as the system transitions between the compressor stages. This offers insights into the

efficacy of insulation during the adiabatic conversion process. An optimal insulation setup would minimize entropy generation, thereby edging the process closer to being adiabatic and well isolated. In this section, I introduce the concept of reversibility, which is subsequently elaborated upon in the dedicated section “Compressor(s) performance analysis”. This analysis offers a comprehensive perspective on the system’s operational efficiency and its alignment with the fundamental principles of thermodynamics.

#### 4.3.1. Refrigeration cycle analysis

The theoretical COP of the heat pump is gleaned from the refrigeration cycle diagrams. The construction of the cycle involved a meticulous point-by-point process, followed by connecting these main points to form a complete cycle. This process and its resultant cycle are vividly illustrated in Figure 28 below.

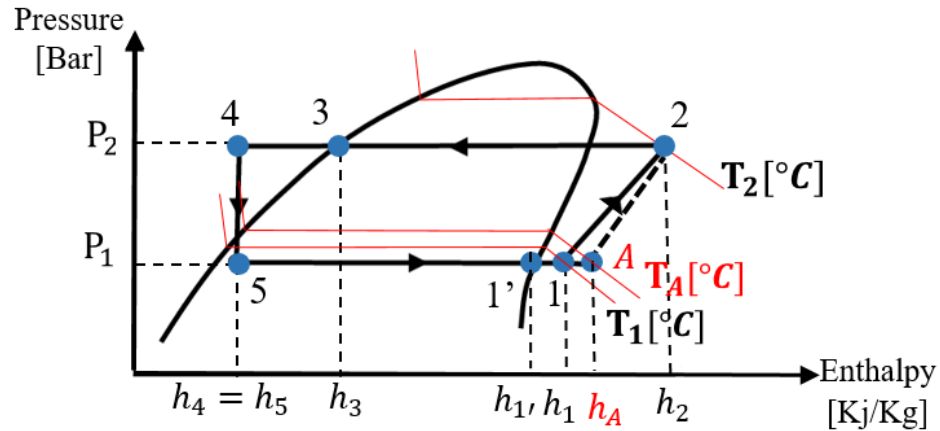


**Figure 28.** Schematic drawing of the experimental setup: (28A) Sample p-h diagram, (28B) Heat pump.

The drawing is executed on a blank P-h diagram for the refrigerant R22, in the CoolPack software. In this p-h diagram, I pinpoint the pressure and temperature data collected from various sensors and instruments. Each scenario is visually depicted on a single graph, with the insulated system highlighted in a distinct green cycle, while the non-insulated one is illustrated in a contrasting black, we placed these graphs in Annex C, and the characteristics of each point are set in tables 15 to 18 below.

In Figure 29 below, Point A in the graph symbolizes the real temperature value corresponding to the measured by the Testo clamp thermometer. The average results are documented in Tables 11

to 14, and the new values are in Tables 15 to 18. It's important to note that the measurement wasn't taken directly at the compressor's inlet (a challenging location to measure precisely), which obliged us to relocate point A to the new point 1, as indicated in Figure 29 below.



**Figure 29.** Theoretical plotting of the cycle.

The  $T_A$  (experimental temperature) compared to  $T_1$  (theoretical temperature) is much higher, as evident from the visual representation in the graph or through a numerical comparison in the referenced tables.

The placement of these points on the p-h diagram is based on the data acquired from our experiment:

- Points 1 and 2: The average pressure results are sourced from the Testo 549i Bluetooth high-pressure gauge, while the temperature data is derived from the Testo 115i Bluetooth clamp thermometer, we assumed that the starting point is at  $1'$  which represents the vapor saturation point at the low-pressure ( $P_1$ ), adding a  $5^\circ C$  of superheating to land in the point 1.
- Point 3: To locate this point we took the average temperature collected from the sensor positioned at the condenser's output (the third channel of the ALMEMO, Model 2590-9, Fig.19). This measurement marks the liquid saturation point.
- Point 4: We presume that the subcooling of the refrigerant has reached the average ambient temperature (gained from the first channel of the same ALMEMO previously indicated).

- Point 5: To plot point 5, we take a direct path, intersecting the lines corresponding to the expansion valve and evaporator processes on the diagram, since no sensors were positioned at the expansion valve output.

Upon identifying these crucial points, we proceeded to establish the connections between them to construct our comprehensive thermodynamic refrigeration cycles, disregarding any form of pressure drops. Utilizing the CoolPack software, I effortlessly obtained the data corresponding to each key point simply by hovering the cursor over them, as depicted in tables 15, 16, 17, and 18 below.

**Table 15.** First day: Thermodynamic cycle data: Non-insulated HP with one operating compressor.

Main points of the cycle	Temp. [°C]	Pressure [bar]	Enthalpy [Kj/Kg]	Volume [m <sup>3</sup> /Kg]	Entropy [Kj/K.Kg]	Vapor quality
1'	-11,20	3,40	400,61	0,06788	1,7675	1
1	-6,20	3,40	404,09	0,06962	1,7806	1
2	76,04	14,66	449,71	0,01979	1,8035	1
3	34,54	13,648	242,5	NA	1,144	0
4	29,22	13,648	236,58	NA	1,123	0
5	-10,567	3,40	236,58	0,01896	1,141	0,246

**Table 16.** Third day: Thermodynamic cycle data: Insulated HP with one operating compressor.

Main points of the cycle	Temp. [°C]	Pressure [bar]	Enthalpy [Kj/Kg]	Volume [m <sup>3</sup> /Kg]	Entropy [Kj/K.Kg]	Vapor quality
1'	-7,29	3,90	402,15	0,05953	1,7613	1
1	-2,29	3,90	405,71	0,06108	1,7745	1
2	73,16	15,93	445,60	0,01767	1,7849	1
3	38,23	15,220	247,31	NA	1,159	0
4	33,23	15,037	241,02	NA	1,139	0
5	-7,111	3,90	241,02	0,01735	1,154	0,232

**Table 17.** Second day: Thermodynamic cycle data: Non-insulated HP with two operating compressors.

Main points of the cycle	Temp. [°C]	Pressure [bar]	Enthalpy [Kj/Kg]	Volume [m <sup>3</sup> /Kg]	Entropy [Kj/K.Kg]	Vapor quality
1'	-18,48	2,60	397,63	0,0876	1,7798	1
1	-13,48	2,60	400,99	0,8979	1,7928	1
2	88,17	17,69	456,49	0,01676	1,8071	1
3	42,04	16,170	252,49	NA	1,175	0
4	36,60	15,975	246,57	NA	1,152	0
5	-17,508	2,60	246,57	0,02948	1,185	0,305

**Table 18.** Fourth day: Thermodynamic cycle data: Insulated HP with two operating compressors.

Main points of the cycle	Temp. [°C]	Pressure [bar]	Enthalpy [Kj/Kg]	Volume [m <sup>3</sup> /Kg]	Entropy [Kj/K.Kg]	Vapor quality
1'	-19,50	2,50	397,21	0,0091	1,7816	1
1	-14,50	2,50	400,55	0,9319	1,7946	1
2	76,47	16,37	447,90	0,01738	1,7893	1
3	38,95	15,220	248,42	NA	1,163	0
4	27,30	15,405	232,88	NA	1,113	0
5	-19,417	2,50	232,88	0,02689	1,135	0,252

#### 4.3.2. Analysis of entropy variations

Before moving in presenting the COP results, Table 19 shows the entropy variation of the cycle between points 1 and 2, signifying the compressor's input and output, respectively. This variation represents the adiabatic conversion and indicates the efficiency of the insulation applied at the level of the compressor(s), where whenever the difference of the entropy  $\Delta S$  ( $S_2 - S_1$ ) approaches zero, the system is more insulated and the conversion is adiabatic ( $S_2 = S_1$ ).

**Table 19.** Entropy variation between compressor(s) input and output points.

Scenarios	$S_1$ [Kj/K. Kg]	$S_2$ [Kj/K. Kg]	$\Delta S = S_2 - S_1$ [Kj/K. Kg]
First day: Non-insulated HP with one operating compressor.	1,7806	1,8035	0,0229
Third day: Insulated HP with one operating compressor.	1,7745	1,7849	0,0104
Second day: Non-insulated HP with two operating compressors.	1,7928	1,8071	0,0143
Fourth day: Insulated HP with two operating compressors.	1,7946	1,7893	-0,0053

On the first day, there was an entropy increase of 0,0229 [Kj/K. Kg]. By the third day, with the HP insulated and still operating one compressor, the entropy variation was reduced by more than half to 0,0104 [Kj/K. Kg]. This substantial reduction indicates that the insulation effectively decreased the entropy change, thereby moving the process closer to an adiabatic condition.

On the second day, the observed entropy change of 0,0143 [Kj/K. Kg] was found to be lower than the entropy change observed while using a single compressor without insulation. Interestingly, on the fourth day, there was a reversal in the direction of entropy variation, indicating a drop of 0,0053 [Kj/K. Kg] (the presence of a negative value can be attributed to the precision of the obtained results), given that the value was the closest to zero, the experiment with two functioning compressors and an insulated setup was adiabatic, indicating that the setup was perfectly insulated.

In the absence of insulation, the entropy change was more pronounced with a single compressor ( $\Delta S = 0,0229$  [Kj/K. Kg]) than with two compressors ( $\Delta S = 0,0143$  [Kj/K. Kg]). This suggests that using two compressors, even without insulation, enhances the thermodynamic efficiency of a system with just one compressor. This trend persists when insulation is added. For insulated systems, the entropy change with one compressor is  $\Delta S = 0,0104$  [Kj/K. Kg], but it further reduces to  $\Delta S = 0,0053$  [Kj/K. Kg] with two compressors. Our findings consistently show that, regardless of insulation, increasing the number of compressors reduces thermodynamic losses.

### 4.3.3. COP results

The following investigation analyzes the impact of two key sections on the COP, the inclusion or exclusion of insulation, and the number of operational compressors, by making a comparison of theoretical and real COPs in various experimental scenarios.

We calculated the theoretical COP for each day using Equation (21) provided below:

$$\text{COP}_{HP_{theor.}} = \frac{\dot{Q}_H}{\dot{W}} = \frac{(h_2 - h_4)}{(h_2 - h_1)} \quad (21)$$

Where  $h_1$ ,  $h_2$ , and  $h_4$  are the enthalpies described in tables 15, 16, 17, and 18 above.

The following equation was used to compute the real COP for each day based on the measured data:

$$\text{COP}_{HP_{real}} = \frac{\dot{Q}_H}{P_{eff}} \quad (22)$$

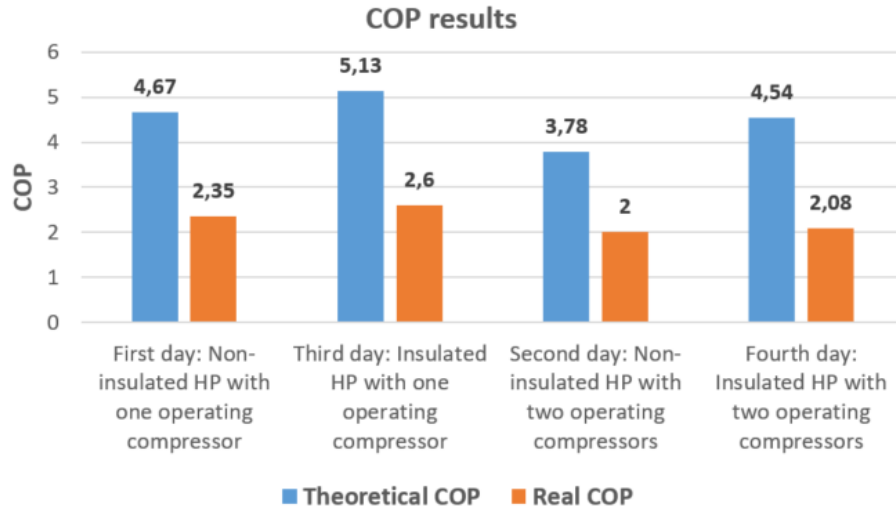
The results are displayed in the following Table 20.

**Table 20.** Theoretical and real COP results over the four measured days.

Scenarios	Theoretical COP	Real COP
First day: Non-insulated HP with one operating compressor.	4,67	2,35
Third day: Insulated HP with one operating compressor.	5,13	2,60
Second day: Non-insulated HP with two operating compressors.	3,78	2,00
Fourth day: Insulated HP with two operating compressors.	4,54	2,08

The findings are visually depicted in Figure 30, followed by a comprehensive discussion that follows the presentation of the chart.





**Figure 30.** Theoretical vs. real COP values: A four-day comparative chart.

#### Effect of the insulation

During the first day, the heat pump without insulation and equipped with a single functioning compressor had a theoretical COP of 4,67. Nevertheless, under experimental settings, it was shown that the obtained value was only 2,35, representing approximately 50% of the theoretical value. The substantial gap seen can be linked to errors within the measurement especially at the suction line (real value of the point 1), heat dissipation, and improper operational parameters. After the application of insulation to the HP, the theoretical COP saw a rise to 5,13 on the third day. Additionally, the real COP showed a little improvement, reaching 2,60.

The aforementioned statement remained consistent during the operation of two compressors, on the second day, with the heat pump lacking insulation, the theoretical COP stood at 3,78, this figure improved to 4,54 once the system was insulated. However, the actual COP values remained disappointingly low, showing only a marginal enhancement: from 2,00 without insulation to 2,08 with insulation. This slight increase contrasts sharply with the significant gap between the real and theoretical outcomes.

#### Effect of the operational compressors

Comparing the first and second days, where the insulation was missing in those days, and the system was operating with one and two compressors respectively, we found that the theoretical

COP dropped from 4,67 to 3,78. Similarly, the real COP also declined from 2,35 to 2,00. The same remark when the insulation was applied, on the fourth day, with insulation and two operating compressors, the theoretical COP was 4,54, which is lower than the single-compressor insulated setup on the third day (5,13). The real COP comparison gives the same remark, where on the fourth day was 2,08 which was higher on the third day (2,60).

The drop in COP values of the heat pump over the discussed scenarios by adding more compressors appears to be affected by other components within the system. Our assessment of the operating compressors revealed that their efficiency improved with the addition of more compressors, as confirmed via the reversibility criteria. However, it should be noted that this study did not directly analyze the evaporator or condenser, so any differences in performance related to these components remain speculative assumptions.

In the two compressor cases, the fact that the physical size of the heat exchangers has not changed, but the cooling circuit capacity has increased, so that the heat exchangers have become relatively undersized, may be responsible for the COP reduction. This may also have caused the differences in suction and discharge pressures: in the case of two compressors delivered from lower to higher pressures, reducing the COP value.

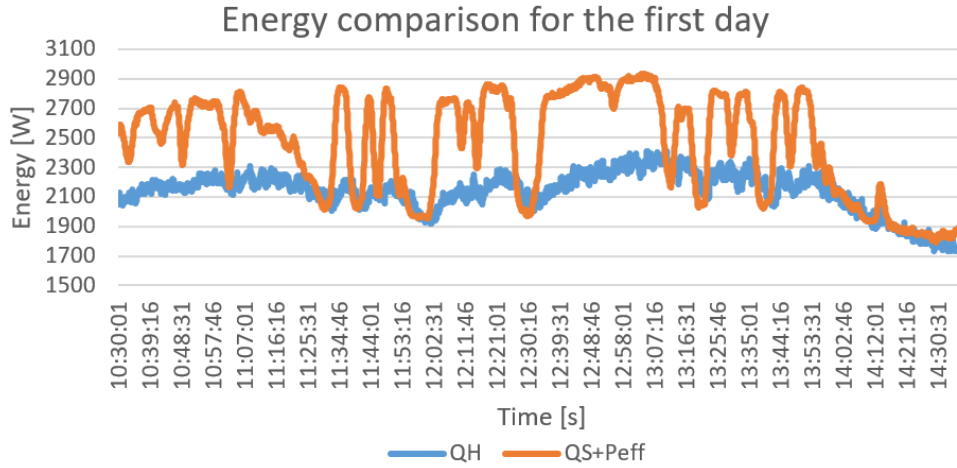
#### **4.4. System energy analysis**

As the energy balance equation cited in equation (15) describes the overall energy distribution, we can note that in an ideal case, the heat acquired from the solar collector ( $\dot{Q}_S$ ), when added to the effective power consumption of the compressor(s) ( $P_{eff}$ ), should perfectly balance with the total heat output of the condenser ( $\dot{Q}_H$ ). However, the attainment of this ideal equilibrium is elusive, necessitating the introduction of a corrective term which is the energy loss by the system ( $E_{loss}$ ). In this evaluation section, we will evaluate the condenser's thermal performance in relation to the energy used by the compressor and extracted heat from the solar plate. We examine system performance in both cases over a period of four measurable days.

##### **4.4.1. For a single compressor scenario (the first and the third day)**

Figure 31 illustrates an energy comparison analysis conducted on the first day, focusing on a scenario where a single compressor is in operation with the absence of insulation. This figure provides valuable insights into the energy consumption by the compressor and energy gained for

the solar plate together in the orange graph ( $\dot{Q}_S + P_{eff}$ ), while the blue graph represents the total thermal energy of the nine sections of the condenser ( $\dot{Q}_H$ ).



**Figure 31.** Energy comparison on the first day: A single compressor operating without insulation.

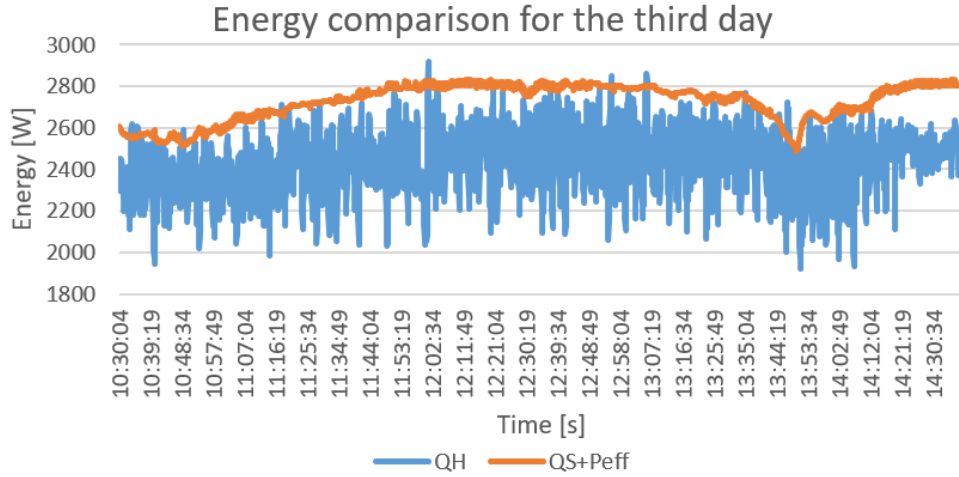
The disparity between the two graphs serves as a visual depiction of the energy losses incurred within our setup. In this specific instance, our system has experienced greater energy losses compared to the energy savings achieved. These energy losses occurred when the graphs were not aligned, a summary of the graphs is displayed in Table 21.

**Table 21.** First day: Average energy loss calculation of one compressor: Non-insulated HP.

Data [W]	Extracted heat ( $\dot{Q}_S$ )	Consumed power ( $P_{eff}$ )	$\dot{Q}_S + P_{eff}$	Total released heat ( $\dot{Q}_H$ )	Energy loss ( $E_{loss}$ ) ( $\dot{Q}_H - \dot{Q}_S - P_{eff}$ )
Avg.	1574	897	2474	2052	-419

The compressor's power consumption remained steady throughout the day, averaging around 900 [W]. Consequently, the energy balance primarily hinges on the correlation between the heat extracted by the solar collector and the total heat of the condenser. This relationship is primarily influenced by the temperature differential between the collector's input and output, which in turn, is closely tied to ambient conditions, particularly solar radiation levels. In light of this observation, it becomes evident that the graphs exhibit alignment when the outlet temperature decreases, as demonstrated in the preceding Figure 24.

On the third day, we made the same experiment where only one compressor was running and we added the insulation, the results are shown in Figure 32, where the two graphs were close to each other and the gap was relatively small compared to Figure 31, this close alignment underscores the insulation's exceptional effectiveness in reducing overall system losses.



**Figure 32.** Energy comparison on the third day: A single compressor operating with insulation.

We also note that the summation of energy consumption and the heat extracted by the solar panel correlates with the outlet temperature of the antifreeze as depicted in Figure 25.

Table 22 provides a concise summary of the findings presented in Figure 32, facilitating a comprehensive comparison of system losses in both scenarios.

**Table 22.** Third day: Average energy loss calculation of one compressor: Insulated HP.

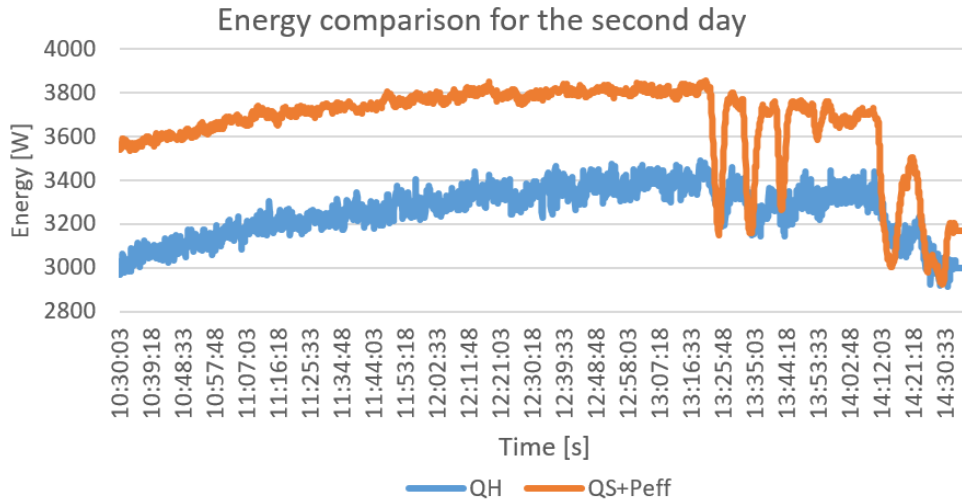
Data [W]	Extracted heat ( $\dot{Q}_S$ )	Consumed power ( $P_{eff}$ )	$\dot{Q}_S + P_{eff}$	Total released heat ( $\dot{Q}_H$ )	Energy loss ( $E_{loss}$ ) ( $\dot{Q}_H - \dot{Q}_S - P_{eff}$ )
Avg.	1774	949	2723	2394	-329

As was previously mentioned, adding insulation reduced system losses from 419 [W] without it to 329 [W]. The insulation resulted in a significant decrease in energy consumption (by 90 [W] in this case). Given that the effect of insulation has already been proven relating to the heat pump, it is significant to recognize the impact of insulation at the other block of our setup which is the solar collector part, where the impact of insulation becomes even more pronounced. Observations indicated that as the outlet temperature rises, leading to increased heat absorption from the solar,

discrepancies emerge (evidenced by the non-alignment of the two curves in the graphs, especially the one in Fig. 31). These discrepancies or losses become starkly apparent in the absence of insulation, emphasizing its indispensable role in ensuring system efficiency across various components.

#### 4.4.2. In a dual-compressor scenario (the second and the fourth day)

The experiment done with the case of the double compressor running gave structurally the same results, the only difference is in the output data where energy consumption registered was higher, and the thermal output of the solar collector and the condenser increased as well. Figure 33 is the case where the system lacks insulation, where the graphs are not aligned with each other due to the existence of the losses.



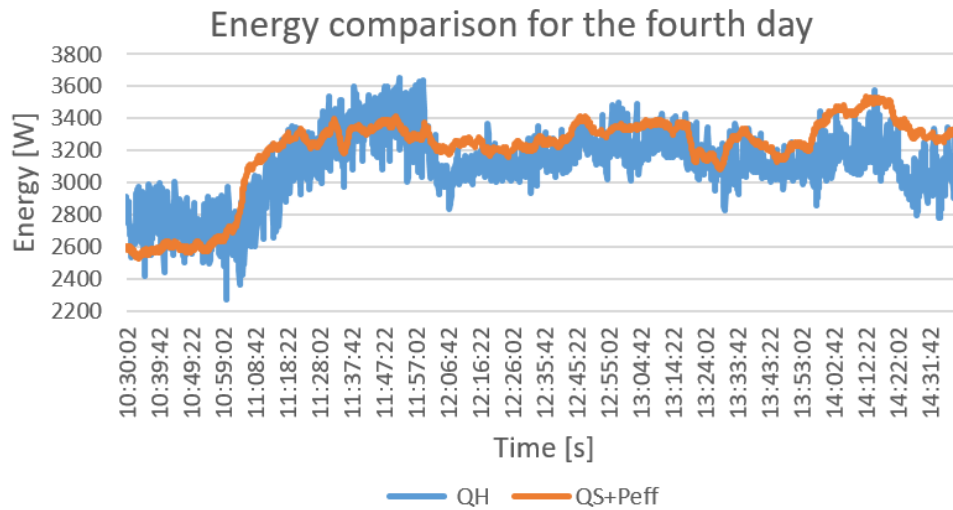
**Figure 33.** Energy comparison on the second day: Two compressors operating without insulation.

The alignment exists when the outlet temperature is dropped, where it was the case shown in Figure 26. The average amount of energy loss is calculated in Table 23 below.

**Table 23.** The second day: Average energy loss calculation of two compressors: Non-insulated HP.

Data [W]	Extracted heat ( $\dot{Q}_S$ )	Consumed power ( $P_{eff}$ )	$\dot{Q}_S + P_{eff}$	Total released heat ( $\dot{Q}_H$ )	Energy loss ( $E_{loss}$ ) ( $\dot{Q}_H - \dot{Q}_S - P_{eff}$ )
Avg.	2044	1632	3676	2970	-706

Figure 34 below clarifies how the results prove the insulation to be exceptionally successful under the working conditions of both compressors. On the fourth day, the system reaches its ideal state where we can see a 0 [W] loss, validating the efficiency of the insulation. As time went on, the two lines remained virtually parallel and aligned throughout the duration of the experiment.



**Figure 34.** Energy comparison on the fourth day: Two compressors operating with insulation.

Table 24 presents the average data extracted from Figure 34, offering a comprehensive view of the average losses in comparison to the non-insulated configuration.

**Table 24.** The fourth day: Average energy loss calculation of two compressors: Insulated HP.

Data [W]	Extracted heat ( $\dot{Q}_S$ )	Consumed power ( $P_{eff}$ )	$\dot{Q}_S + P_{eff}$	Total released heat ( $\dot{Q}_H$ )	Energy loss ( $E_{loss}$ ) ( $\dot{Q}_H - \dot{Q}_S - P_{eff}$ )
Avg.	1691	1500	3191	2914	-277

The recorded overall energy loss amount is 277 [W] marking a significant reduction compared to any prior instances, irrespective of whether one compressor was operating or both, insulated or not. Notably, when both compressors are running concurrently and insulation is introduced, substantial energy savings of 429 [W] were achieved. From these observations, it's evident that increasing the number of compressors reduces energy loss, and this efficiency is further enhanced when the system is properly insulated.

## **5. Recommendations and future work**

The experimental results indicate that the measured range of Coefficient of Performance (COP) values was quite small, spanning from 2 to 2,6. This finding is in opposition to the theoretical outcomes, which repeatedly demonstrated greater coefficients of performance (COP) ranging from 3,78 to 5,13. The variation in COP outcomes can be attributed mostly to the accuracy of our measurements, particularly in the modeling phase using the CoolPack program, as well as the unquantified losses inherent in the system, particularly at the evaporator and solar collector. Hence, the author proposes the integration of a more thorough energy analysis into comparable systems to achieve improved precision and reliability as follows:

- Fluid dynamics analysis: In the context of our thermal integration system, the evaporator plays a crucial role as a heat exchanger. Therefore, knowing the refrigerant flow rate would help to compare the thermal energy gained from the solar collector through the antifreeze, and the absorbed heat from the refrigerant. This analysis effectively allows for the identification and mitigation of potential losses occurring at the evaporator stage.
- Pressure and temperature drops in the heat pump: In this work, temperature and pressure drops were not considered due to the absence of the necessary measuring instruments and to simplify the evaluation process. However, for a comprehensive assessment and accurate system performance, it's essential to account for these drops in future studies.
- System integration with smart controls: Integrate the SAHP with a smart control system that can adjust the compressor's operation based on real-time environmental conditions, optimizing energy consumption and output simultaneously.
- Insulation materials: While rubber and inorganic fibrous materials were utilized in this study, future work might explore the use of advanced aerogel insulations or vacuum-

insulated panels (VIPs). These materials have shown superior thermal insulating properties and could potentially enhance the system's efficiency further.

- Hybrid energy sources: In situations where there is a decrease in the availability of solar energy, the addition of an auxiliary energy source such as geothermal can ensure the continued effectiveness of the system. This phenomenon is demonstrated in a pertinent study (Reference 44), whereby an examination was conducted on a ground-assisted heat pump system. The study's findings closely corresponded with our own, as evidenced by the reported coefficient of performance (COP) values, which ranged from 2,00 to 3,125. This highlights the importance of implementing a diversified portfolio of energy sources in order to ensure the stability of the system in the face of changing conditions.
- Project revenue and Break-even analysis: The findings of this study suggest that operating a system with multiple compressors enhances efficiency and reduces energy losses. However, the decision to use more than one compressor largely depends on the project's objectives and requirements. A financial analysis can provide clarity on whether incorporating additional units is a cost-effective choice or not.



## 6. Conclusion

In my research, conducted at the energetic building's laboratory of the Hungarian University of Agriculture and Life Sciences, I analyzed the thermodynamic and energy dynamics of a Solar Assisted Heat Pump (SAHP). Spanning over four days, the experiment aimed to study the influences of insulation on the SAHP and discern how these could be leveraged for optimal heating applications. Central to our energetic investigation was the heat pump's compressor, specifically, a twin-compressor model. On certain days, we engaged both compressors, while on others, only one was in operation. To bolster our findings, we employed an inorganic fibrous material to envelop the compressors and used rubber insulation for the heat pump tubes and the conduits connected to the solar collector, thereby gauging the efficacy of these insulation measures on the system's performance.

The evaluation begins by examining the integration of the solar collector and the ambient factors that affect the system. Our findings indicate that the solar plate demonstrates efficient harnessing and utilization of solar energy, even under adverse environmental circumstances. The ability to withstand and adapt to changing external influences demonstrates the capacity to maximize the usage of solar energy in a given system, regardless of the current environmental conditions. To fully and fairly compare insulated and uninsulated designs, I found that it is important to be aware of how external factors can make it hard to tell what effect insulation has, significant findings warrant attention summarized in the following key points:

- The results presented in Tables 7 and 8 indicate that higher ambient temperatures led to increased temperatures of the mixture both before and after, but the increase in temperature difference lagged behind the increase in global warming. This discrepancy might be attributed to the limitations of the compressor, which prevented achieving a cooling capacity sufficient to maintain the outlet mixture temperature at the level indicated in Table 7. This phenomenon may also affect the results for the other measurement days.
- The temperature difference was larger with two compressors (Tables 9 and 10) than with one compressor, as the cooling capacity was also higher. However, the increase in compressor power was not proportional to the heat power extracted. The difference here is

in the temperature levels of the inlet and outlet of the mixture in all cases, lower values were recorded than in the single compressor cases.

- From the data in Tables 13 and 14, it can be seen that the compressor outlet temperature is lower in the insulated case. This can be explained by the change in ambient conditions (Tables 9 and 10), i.e. lower global radiation and lower ambient temperature result in lower compressor outlet temperature even with insulation.

By looking more closely at how the compressor works, we found that insulation really helps move the system toward a perfect, reversible state by reducing the loss of energy due to exterior thermal transformation. Furthermore, our findings indicated that for an insulated system to work at its best, both the quality of the insulation and the proper handling of the compressor's workload must be carefully planned. The reliability of these results was further proven by looking at the changes in entropy of the refrigerant before and after it went through the compressor(s). Our data showed a consistent pattern: using more compressors always reduced thermodynamic losses, no matter if insulation was present or not.

In the presented study, we've compared the experimentally measured Coefficient of Performance (COP) with its corresponding theoretical value, which was calculated using the CoolPack software. Significantly, the apparent advantages of insulation in enhancing the efficiency of the heat pump appeared to be stronger in theoretical projections than in real results. Furthermore, it is evident that there is a noticeable decrease in the COP values in different scenarios, especially when operating both compressors. This implies that there may be potential factors from other components of the heat pump that are affecting the COP amounts. This statement highlights the complex nature of system performance, suggesting that while insulation and compressor functioning are crucial factors, there are additional components inside the system that significantly influence overall efficiency.

Following further examination at Table 19 which summarizes the entropy variation, we found that the insulation significantly reduced the entropy changes of the system at the level of the compressor, evidenced by a decrease from 0,0229 [Kj/K. Kg] to 0,0104 [Kj/K. Kg] with one compressor. With two compressors, even without insulation, improved thermodynamic efficiency, with entropy changes dropping from 0,0229 [Kj/K. Kg] to 0,0143 [Kj/K. Kg]. Adding insulation further lowered entropy changes, reaching 0,0053 [Kj/K. Kg] with two compressors, suggesting

enhanced efficiency and reduced thermodynamic losses with multiple compressors and with applied insulation.

Upon evaluating the system's overall energy losses, a clear association was observed between the outlet temperature of the solar collector and the overall energy losses. Specifically, it was determined that a decrease in the outlet temperature resulted in a reduction in the amount of heat gained and subsequently led to lowered system losses. Furthermore, the obtained results have once again confirmed our previous findings, demonstrating that the increase in the number of compressors consistently leads to a decrease in energy losses. Significantly, the enhancement in efficiency resulting from the utilization of additional compressors was amplified when the system was appropriately insulated. The interdependence of insulation and compressor operation forms the foundation for the critical function that both components fulfill in optimizing system efficiency and reducing energy inefficiencies.

## Summary

In a world grappling with the ever-growing demand for energy, the importance of devising sustainable and efficient energy solutions has never been more paramount. As non-renewable resources deplete and the consequences of greenhouse gas emissions become increasingly evident, the shift towards renewable energy sources becomes not just preferable, but essential. Among these sources, solar energy stands out as one of the most abundant and untapped potentials.

The Solar Assisted Heat Pump (SAHP), as explored in our study, emerges as a beacon in this renewable energy landscape, particularly for heating and cooling applications. Its ability to combine the natural and limitless power of the sun with modern thermodynamic principles offers a promising avenue to not just harness but also optimize this energy. Our research, conducted at the energetic building's laboratory of the Hungarian University of Agriculture and Life Sciences, delved deep into the intricacies of the SAHP, focusing on the dynamics of insulation and compressor operation. Through systematic experiments and comprehensive analysis, we unearthed valuable insights into the operational efficiency of the SAHP, especially in fluctuating environmental conditions. As heating remains one of the main energy needs across global households and industries around the world, the potential applications and benefits of a well-designed SAHP system become apparent and essential. This not only translates into tangible cost savings but also contributes significantly to reducing carbon footprints, aligning with the global push for sustainable living.

To conclude, energy stands as the cornerstone of modern civilization, and as we move forward, innovations like the Solar Assisted Heat Pump serve as exemplary models of how we can align our energy needs with the preservation and health of our planet.

## DECLARATION

### on authenticity and public assess of final mater's thesis

Student's name: Herzallah Lazhari  
Student's Neptun ID: TICYFS  
Title of the document: Energetic investigation of a compressor refrigeration cycle  
Year of publication: 2023  
Department: Mechanical Engineering

I declare that the submitted master's thesis is my own, original individual creation. Any parts taken from an another author's work are clearly marked, and listed in the table of contents.

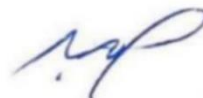
If the statements above are not true, I acknowledge that the Final examination board excludes me from participation in the final exam, and I am only allowed to take final exam if I submit another master's thesis.

Viewing and printing my submitted work in a PDF format is permitted. However, the modification of my submitted work shall not be permitted.

I acknowledge that the rules on Intellectual Property Management of Hungarian University of Agriculture and Life Sciences shall apply to my work as an intellectual property.

I acknowledge that the electric version of my work is uploaded to the repository sytem of the Hungarian University of Agriculture and Life Sciences.

Place and date: Gödöllő, 2023 November 01



---

Student's signature

## STATEMENT ON CONSULTATION PRACTICES

As a supervisor of Herzallah Lazhari TICYFS, I here declare that the master's thesis has been reviewed by me, the student was informed about the requirements of literary sources management and its legal and ethical rules.

**I recommend**/don't recommend the master's thesis to be defended in a final exam.

The document contains state secrets or professional secrets: yes      **no**

Place and date: Gödöllő, 2023 November 01



Internal supervisor

## Bibliography

- [1]. Omer, A. M. (2008). Ground-source heat pumps systems and applications. *Renewable and sustainable energy reviews*, 12(2), 344-371.
- [2]. Carroll, P., Chesser, M., and Lyons, P. (2020). Air Source Heat Pumps field studies: A systematic literature review. *Renewable and sustainable energy reviews*, 134, 110275.
- [3]. Thomas, N. (2015). *Westring Pascal. European heat pump market and statistics report 2015*. Technical report. Brussels: The European Heat Pump Association AISBL (EHPA).
- [4]. Vorushylo, I., Keatley, P., Shah, N., Green, R., and Hewitt, N. (2018). How heat pumps and thermal energy storage can be used to manage wind power: A study of Ireland. *Energy*, 157, 539-549.
- [5]. Baxter, V. D., Rice, C. K., Munk, J. D., Ally, M. R., Shen, B., and Uselton, R. B. (2017). *Air-Source Integrated Heat Pump System Development–Final Report* (No. ORNL/TM-2017/305; CRADA/NFE-07-01094). Oak Ridge National Lab.(ORNL), Oak Ridge, TN (United States).
- [6]. Le, K., Huang, M., and Hewitt, N. (2018, July). Domestic High Temperature Air Source Heat Pump: Performance Analysis Using TRNSYS Simulations. In *5th International High Performance Buildings Conference at Purdue*.
- [7]. Danielski, I., Fröling, M., and Joelsson, A. (2012). Air source heat pumps and their role in the Swedish energy system. In *Conference on the Greening of Industry Network, GIN 22-24 October 2012, Linköping, Sweden*.
- [8]. Brown, M., Burke-Scoll, M., and Stebnicki, J. (2011). Air source heat pump efficiency gains from low ambient temperature operation using supplemental electric heating. *Financing Energy Improvements*.
- [9]. Çakır, U., Çomaklı, K., Çomaklı, Ö., and Karşlı, S. (2013). An experimental exergetic comparison of four different heat pump systems working at same conditions: As air to air, air to water, water to water and water to air. *Energy*, 58, 210-219.
- [10]. Wang, R. Z., Jin, Z. Q., Zhai, X. Q., Jin, C. C., Luo, W. L., and Eikevik, T. M. (2018). Investigation of annual energy performance of a VWV air source heat pump system. *International Journal of Refrigeration*, 85, 383-394.
- [11]. Air to air heat pump buying guide, <https://www.manomano.co.uk/advice/air-to-air-heat-pump-buying-guide-9996>

- [12]. Terlizzese, T., and Zanchini, E. (2011). Economic and exergy analysis of alternative plants for a zero carbon building complex. *Energy and Buildings*, 43(4), 787-795.
- [13]. Torekov, M. S., Bahnsen, N., and Qvale, B. (2007). The relative competitive positions of the alternative means for domestic heating. *Energy*, 32(5), 627-633.
- [14]. James. (n.d.). How An Air Source Heat Pump Works (With Real Example). <https://sourceheatpump.com/how-an-air-source-heat-pump-works/>
- [15]. Cheung, H., and Braun, J. E. (2014). Performance comparisons for variable-speed ductless and single-speed ducted residential heat pumps. *International journal of refrigeration*, 47, 15-25.
- [16]. Ueno, K., and Loomis, H. (2015). *Long-term monitoring of mini-split ductless heat pumps in the Northeast* (No. DOE/GO-102015-4529). Building Science Corporation, Westford, MA (United States).
- [17]. Hlavinka, A. N., Mjelde, J. W., Dharmasena, S., and Holland, C. (2016). Forecasting the adoption of residential ductless heat pumps. *Energy Economics*, 54, 60-67.
- [18]. Lam, J. C., and Chan, W. W. (2003). Energy performance of air-to-water and water-to-water heat pumps in hotel applications. *Energy conversion and Management*, 44(10), 1625-1631.
- [19]. O'Hegarty, R., Kinnane, O., Lennon, D., and Colclough, S. (2022). Air-to-water heat pumps: Review and analysis of the performance gap between in-use and product rated performance. *Renewable and Sustainable Energy Reviews*, 155, 111887.
- [20]. IEA, U. (2019). Global status report for buildings and construction 2019. *UN Environment programme*, 224.
- [21]. Géczi, G., Bense, L., and Korzenszky, P. (2014). Water tempering of pools using air to water heat pump environmental friendly solution. *Rocznik Ochrona Środowiska*, 16.
- [22]. Dongellini, M., Naldi, C., and Morini, G. L. (2015). Seasonal performance evaluation of electric air-to-water heat pump systems. *Applied Thermal Engineering*, 90, 1072-1081.
- [23]. Hepbaslia, A., and Kalinci, Y. (2008). A review of heat pump water heating systems. *Renew Sustain Energy Rev.*
- [24]. Moriarty, P., and Honnery, D. (2016). Can renewable energy power the future?. *Energy policy*, 93, 3-7.
- [25]. Oh, S., Cho, Y., and Yun, R. (2014). Raw-water source heat pump for a vertical water treatment building. *Energy and buildings*, 68, 321-328.



- [26]. Kim, M. H., Lee, D. W., Yun, R., and Heo, J. (2017). Operational energy saving potential of thermal effluent source heat pump system for greenhouse heating in jeju. *International Journal of Air-Conditioning and Refrigeration*, 25(04), 1750030.
- [27]. Zhu, N., Hu, P., Wang, W., Yu, J., and Lei, F. (2015). Performance analysis of ground water-source heat pump system with improved control strategies for building retrofit. *Renewable energy*, 80, 324-330.
- [28]. Jung, Y., Oh, J., Han, U., and Lee, H. (2022). A comprehensive review of thermal potential and heat utilization for water source heat pump systems. *Energy and Buildings*, 266, 112124.
- [29]. Pump, H. (2009). Heating and Cooling With a Heat Pump.
- [30]. Actimage. (n.d.). Pompe à chaleur eau eau : définition, fonctionnement et avantages. <https://www.dedietrich-thermique.fr/pompe-a-chaleur-tout-savoir-sur-les-differentes-technologies/la-pompe-a-chaleur-eau-eau-definition-fonctionnement-et-avantages>
- [31]. Water-Water heat pumps | Geowatt Kft. (n.d.). <https://geowatt.hu/en/termek/water-water-heat-pumps/>
- [32]. Sauty, J. P., and Ausseur, J. Y. (1985). L'exploitation hydrothermique des nappes par pompe à chaleur eau-eau. *La Houille Blanche*, (3-4), 289-298.
- [33]. Gagneja, A., and Pundhir, S. (2016). Heat pumps and its applications. *International Journal of Advances in Chemical Engineering and Biological Sciences*, 3(1), 117-120.
- [34]. Omer, A. M. (2008). Ground-source heat pumps systems and applications. *Renewable and sustainable energy reviews*, 12(2), 344-371.
- [35]. Philippacopoulos, A. J., and Berndt, M. L. (2001). Influence of debonding in ground heat exchangers used with geothermal heat pumps. *Geothermics*, 30(5), 527-545.
- [36]. Sarbu, I., and Sebarchievici, C. (2014). General review of ground-source heat pump systems for heating and cooling of buildings. *Energy and buildings*, 70, 441-454.
- [37]. Valizade, L. (2013). Ground source heat pumps. *Journal of Clean Energy Technologies*, 1(3), 216-219.
- [38]. Malinovski, S. (2017). Energiatehnoloogiate efektiivsuse võrdlus (Master's thesis, Eesti Maailikool).
- [39]. Geothermal heat pumps. (n.d.). Energy.gov.<https://www.energy.gov/energysaver/geothermal-heat-pumps>


- [40]. Korzenszky, P. (2022). Linear model of DHW system using response surface method approach. *Tehnički vjesnik*, 29(1), 66-72.
- [41]. Nuntaphan, A., Chansena, C., and Kiatsiriroat, T. (2009). Performance analysis of solar water heater combined with heat pump using refrigerant mixture. *Applied Energy*, 86(5), 748-756.
- [42]. Beccali, M., Finocchiaro, P., and Nocke, B. (2009). Energy and economic assessment of desiccant cooling systems coupled with single glazed air and hybrid PV/thermal solar collectors for applications in hot and humid climate. *Solar energy*, 83(10), 1828-1846.
- [43]. Zhang, P., Rong, X., Yang, X., and Zhang, D. (2019). Design and performance simulation of a novel hybrid PV/T-air dual source heat pump system based on a three-fluid heat exchanger. *Solar energy*, 191, 505-517.
- [44]. Ozgener, O., and Hepbasli, A. (2007). A review on the energy and exergy analysis of solar assisted heat pump systems. *Renewable and Sustainable energy reviews*, 11(3), 482-496.
- [45]. Fan, Y., Zhao, X., Han, Z., Li, J., Badiei, A., Akhlaghi, Y. G., and Liu, Z. (2021). Scientific and technological progress and future perspectives of the solar assisted heat pump (SAHP) system. *Energy*, 229, 120719.
- [46]. Sarbu, I., and Sebarchievici, C. (2013). Review of solar refrigeration and cooling systems. *Energy and buildings*, 67, 286-297.
- [47]. Grassi, W. (2017). *Heat pumps: fundamentals and applications*. Springer.
- [48]. Rosen, M. A., and Dincer, I. (2003). Exergy methods for assessing and comparing thermal storage systems. *International Journal of Energy Research*, 27(4), 415-430.
- [49]. Koelet, P. C., Gray, T. B., Koelet, P. C., and Gray, T. B. (1992). Principles of Refrigeration. *Industrial Refrigeration: Principles, Design and Applications*, 1-21.
- [50]. Grassi, W., and Grassi, W. (2018). Types of Compression Heat Pumps and Their Main Components. *Heat Pumps: Fundamentals and Applications*, 15-71.
- [51]. Anbarasu, T., and Pavithra, S. (2011, July). Vapour compression refrigeration system generating fresh water from humidity in the air. In *International Conference on Sustainable Energy and Intelligent Systems (SEISCON 2011)* (pp. 75-79). IET.
- [52]. Khedari, J., Permchart, W., Pratinthong, N., Thepa, S., and Hirunlabh, J. (2001). Field study using the ground as a heat sink for the condensing unit of an air conditioner in Thailand. *Energy*, 26(8), 797-810.

- [53]. Ricardo Costa, N., and Garcia, J. (2015). Applying design of experiments to a compression refrigeration cycle. *Cogent Engineering*, 2(1), 992216.
- [54]. Workbook, E. (2021b, September 30). What is Expansion Valve? Explanation, Function and Types - ElectricalWorkbook. ElectricalWorkbook. <https://electricalworkbook.com/expansion-valve/>
- [55]. Dincer, I. (2017). *Refrigeration systems and applications*. John Wiley and Sons.
- [56]. McLinden, M. O., and Huber, M. L. (2020). (R) Evolution of refrigerants. *Journal of Chemical and Engineering Data*, 65(9), 4176-4193.
- [57]. Stoecker, W. F. (1998). *Industrial refrigeration handbook*. McGraw-Hill Education.
- [58]. Hernandez III, A. C., and Fumo, N. (2020). A review of variable refrigerant flow HVAC system components for residential application. *International Journal of Refrigeration*, 110, 47-57.
- [59]. Vuppaladadiyam, A. K., Antunes, E., Vuppaladadiyam, S. S. V., Baig, Z. T., Subiantoro, A., Lei, G., ... and Duan, H. (2022). Progress in the development and use of refrigerants and unintended environmental consequences. *Science of the Total Environment*, 153670.
- [60]. Calm, J. M., and Hourahan, G. C. (2011, August). Physical, safety, and environmental data for current and alternative refrigerants. In *Proceedings of 23rd international congress of refrigeration (ICR2011), Prague, Czech Republic* (pp. 21-26).
- [61]. Coquelet, C. (2003). *Étude des fluides frigorigènes: mesures et modélisations* (Doctoral dissertation, École Nationale Supérieure des Mines de Paris).
- [62]. Froid, D. U., and REFRIGERATION, O. (2001). Classification of refrigerants. *Int. Inst. Refrig., no. Cl*, 3(2), 1-6.
- [63]. Hermanucz, P. (2022). The effect of changing the refrigerant on the energetic characteristics of the heat pump. *Journal of Central European Green Innovation*, 10 (Suppl 1), 123-134.
- [64]. Lee, M. Y., and Lee, D. Y. (2013). Review on conventional air conditioning, alternative refrigerants, and CO2 heat pumps for vehicles. *Advances in Mechanical Engineering*, 5, 713924.
- [65]. Pal, A., Uddin, K., Thu, K., and Saha, B. B. (2018). Environmental assessment and characteristics of next generation refrigerants.
- [66]. Hermanucz, P., Geczi, G., and Barotfi, I. (2022). Energy efficient solution in the brewing process using a dual-source heat pump. *Thermal Science*, 26(3 Part A), 2311-2319.
- [67]. Leff, H. S. (2018). Reversible and irreversible heat engine and refrigerator cycles. *American Journal of Physics*, 86(5), 344-353.

- [68]. Kosoy, B. V. (2003). Thermodynamics and design principles of refrigeration systems. *Low Temperature and Cryogenic Refrigeration*, 5-22.
- [69]. Cengel, Y.A. and Boles, M.A. (2006) Thermodynamics: An Engineering Approach. Fifth Edition, McGraw Hill, New York.
- [70]. Ochkov, V., Orlov, K., Voloshchuk, V., and Rogalev, N. (2016). *Thermal Engineering Studies with Excel, Mathcad and Internet* (p. 432). Springer International Publishing.
- [71]. Yu, J., Zhao, H., and Li, Y. (2008). Application of an ejector in autocascade refrigeration cycle for the performance improvement. *International journal of refrigeration*, 31(2), 279-286.
- [72]. Selbaş, R., Kızıllan, Ö., and Şencan, A. (2006). Thermoeconomic optimization of subcooled and superheated vapor compression refrigeration cycle. *Energy*, 31(12), 2108-2128.
- [73]. She, X., Yin, Y., and Zhang, X. (2014). A proposed subcooling method for vapor compression refrigeration cycle based on expansion power recovery. *International journal of refrigeration*, 43, 50-61.
- [74]. Sumeru, K., Sukri, M. F., Falahuddin, M. A., and Setyawan, A. (2019). A review on subcooling in vapor compression refrigeration cycle for energy saving. *Jurnal Teknologi*, 81(5).
- [75]. Tritjahjono, R. I., Sumeru, K., Setyawan, A., and Sukri, M. F. (2019). Evaluation of subcooling with liquid-suction heat exchanger on the performance of air conditioning system using R22/R410A/R290/R32 as refrigerants. *Journal of Advanced Research in Fluid Mechanics and Thermal Sciences*, 55(1), 1-11.
- [76]. Klein, S. A. (1992). Design considerations for refrigeration cycles. *International Journal of Refrigeration*, 15(3), 181-185.
- [77]. Dincer, I. (Ed.). (2018). *Comprehensive energy systems*. Elsevier.
- [78]. Hermanucz, P., Géczi, G., and Barótfi, I. (2021). Modeling and measurement methods for multi-source heat pumps. *Science, Technology and Innovation*, 14(3).

## Attachments

### Annex A. Si Global Radiation Sensor



**THEODOR FRIEDRICHS**  
Precise in all conditions

**6003.0000 BG**

**Si Global Radiation Sensor**

GROUP 6  
NO  
VERSION / DATE

RADIATION  
**6003.0000**  
04 / 03.2015

**Connection plan**  
2.5 m on fixed cable:

**Version 6003.1000, 0 ... 5 V**

1	white	Supply Vcc / U <sub>s</sub>
2	brown	GND
3	green	Signal GS

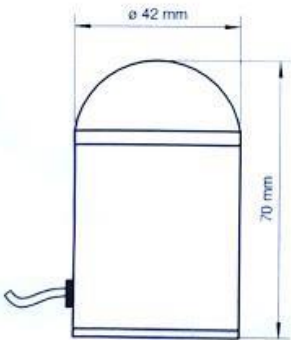
**Version 6003.2000, 4 ... 20 mA**

1	white	Supply Vcc / U <sub>s</sub>
2	brown	GND

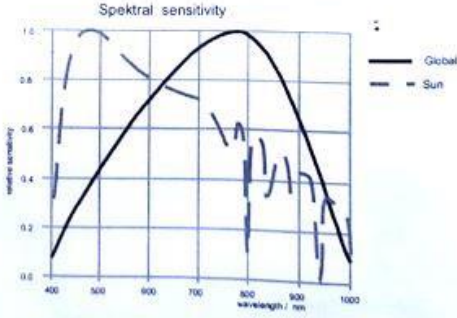
**Version 6000.3000, 0 ... 10 V**

1	white	Supply Vcc / U <sub>s</sub>
2	brown	GND
3	grey	GND
3	yellow	Output

**Dimensions**



**Diagram**



Technical data are subject to change!

THEODOR FRIEDRICHS & CO. | Meteorologische Geräte und Systeme GmbH  
KONTAKT | P +49 (0) 40 839 600 - 0 | F +49 (0) 40 839 600 - 18 | E info@th-friedrichs.de

2 / 2

## Si Global Radiation Sensor

GROUP 6

RADIATION

NO.

**6003.0000**

VERSION / DATE / NAME 04 / 03.2015 / KI



### Description

The Sensor measures the global radiation, basing on a silicon diode with diffusor and PMMA-dome. Especially suitable as reference for photovoltaic systems, including built-in measuring amplifier.

The measuring results are allowing conclusions about medical and biological connections comparing to other spectral ranges.

The measuring head can be used in medical and biological research, in weather information and forecast systems, in climate research, in the agriculture and for public information in general.

### Technical Data

Meas. Range:	0...1.300 W/m <sup>2</sup>		
Spectr. Sensitivity:	380 nm...1.100 nm		
max. Sensitivity at:	780 nm		
Operating Temp.:	-20... +60 °C		
Output:	6003.1000: 0...5 V	6003.2000: 4...20 mA	6003.3000: 0...10 V
Power Supply:	9...30 VDC		
Diffusor:	PTFE		
Dome:	PMMA (UV- pervious)		
Cosinus Correction:	f2 < 6 %		
Linearity:	6003.1000: < 5 %	6003.2000: < 5 %	6003.3000: < 3 %
Absolute Error:	< 10 %		
Dimensions:	Ø 42 x 70 mm		
Weight:	approx. 100 g		

### Ordering Code

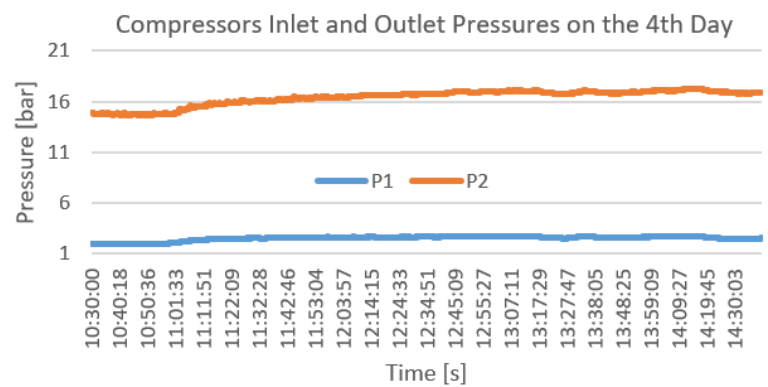
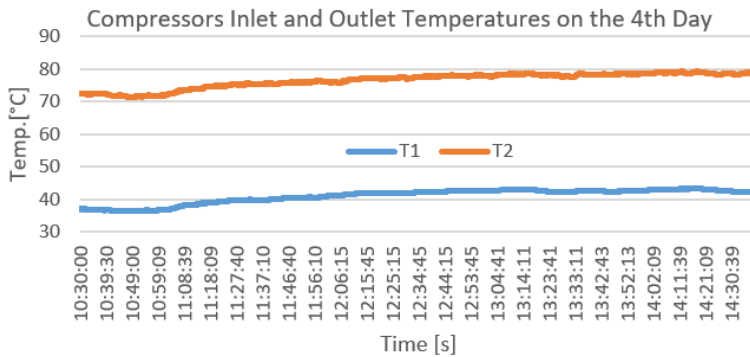
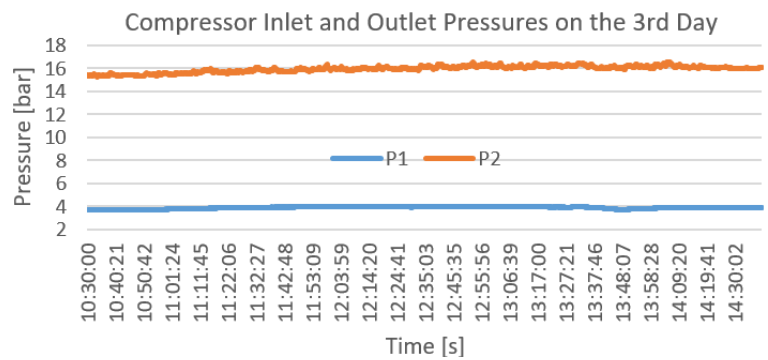
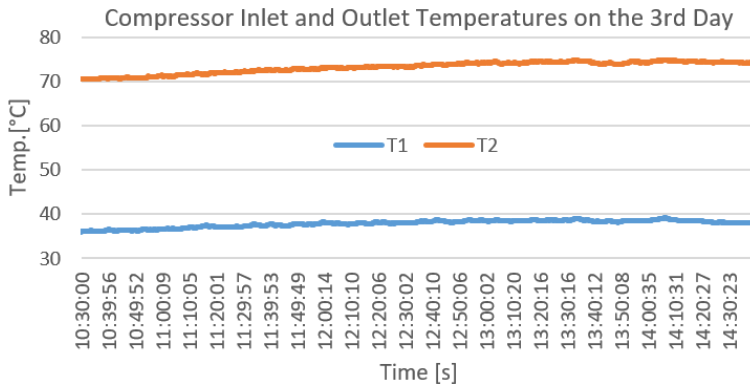
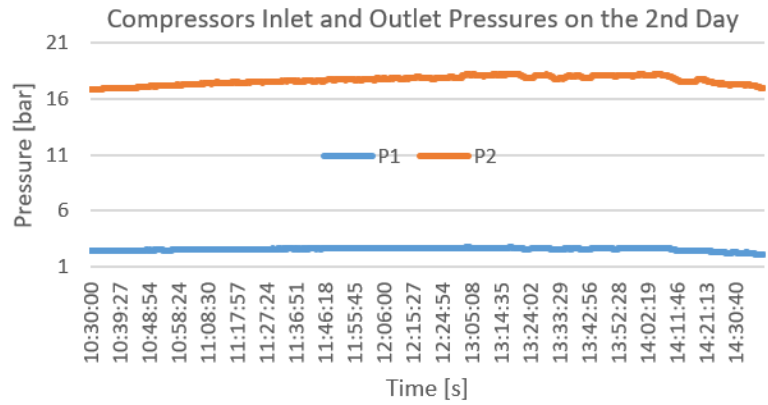
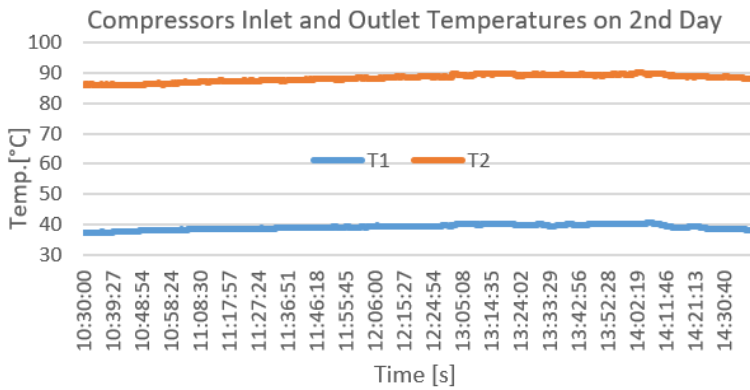
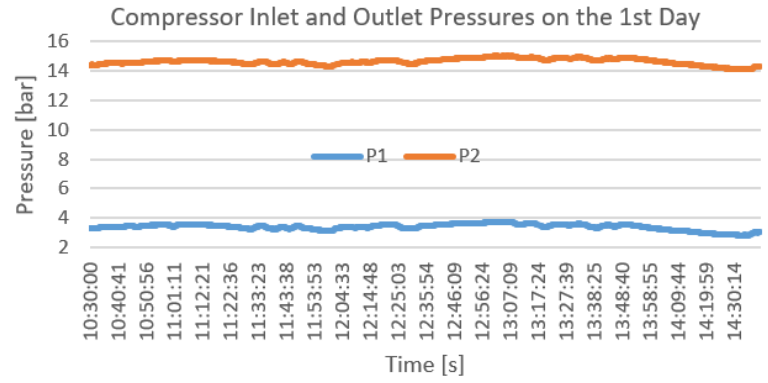
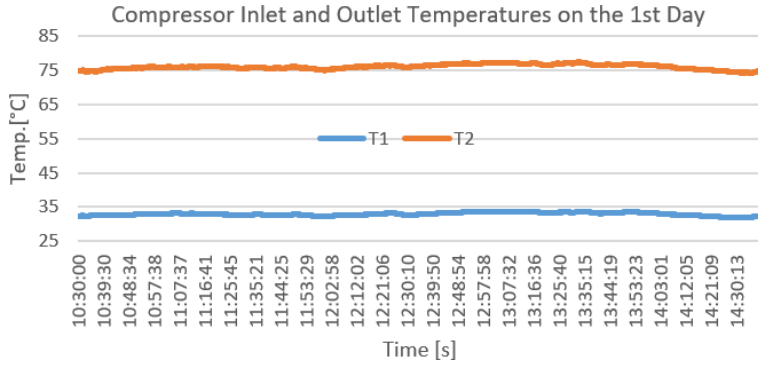
Si-Global Radiation Sensor,	output 0...5 V	<b>6003.1000</b>
Si-Global Radiation Sensor,	output 4...20 mA	<b>6003.2000</b>
Si-Global Radiation Sensor	output 0...10 V	<b>6003.3000</b>

Technical data are subject to change!

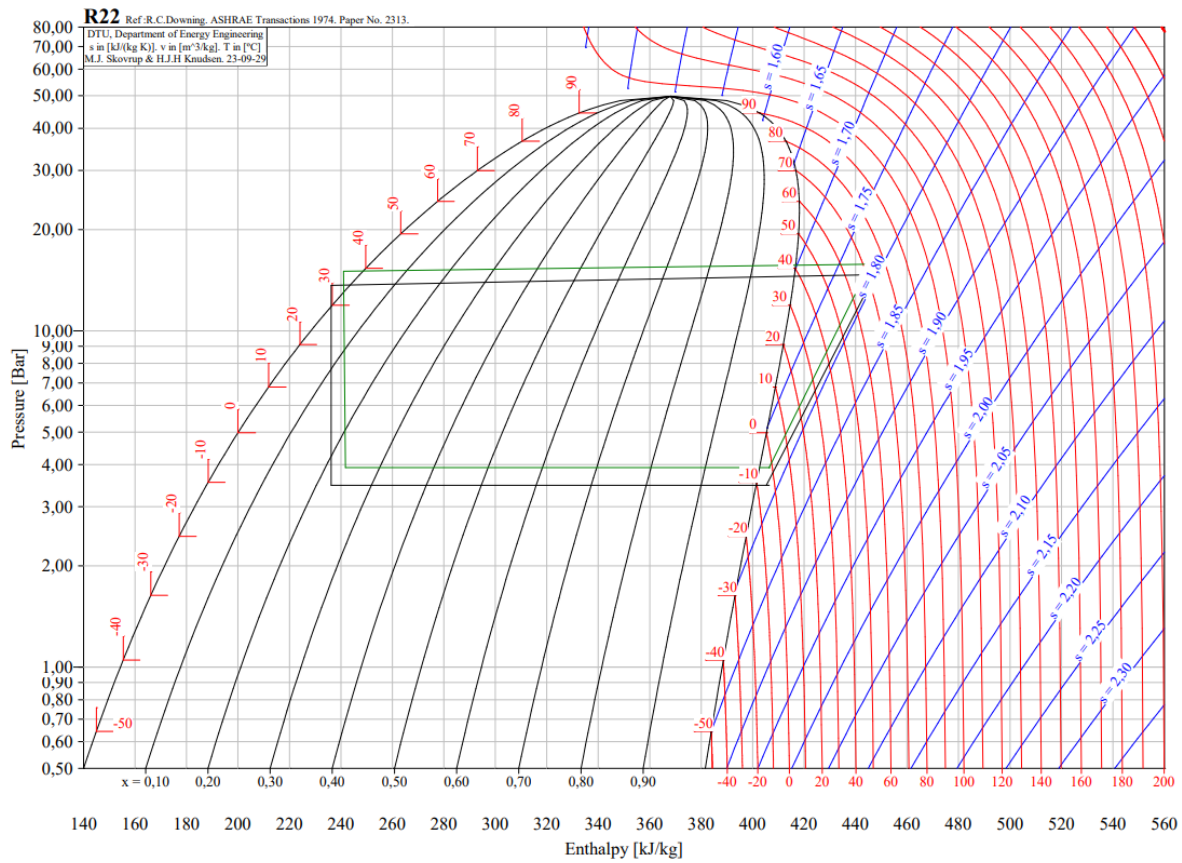
THEODOR FRIEDRICHS & CO. | Meteorologische Geräte und Systeme GmbH  
KONTAKT | P +49 (0) 40 839 600 - 0 | F +49 (0) 40 839 600 - 18 | E info@th-friedrichs.de

1 / 2

## Annex B. Compressor(s)'s measured parameters.

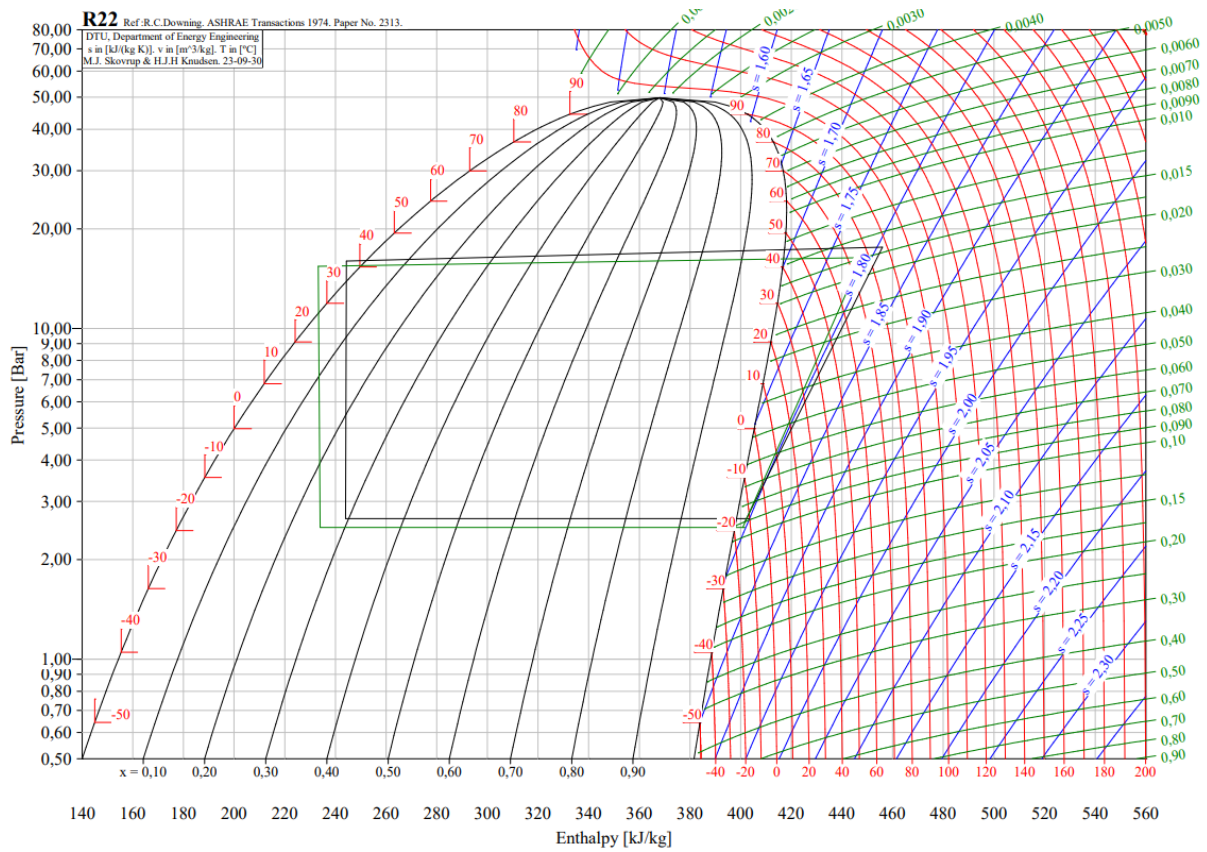


## Annex C. Thermodynamic cycles.



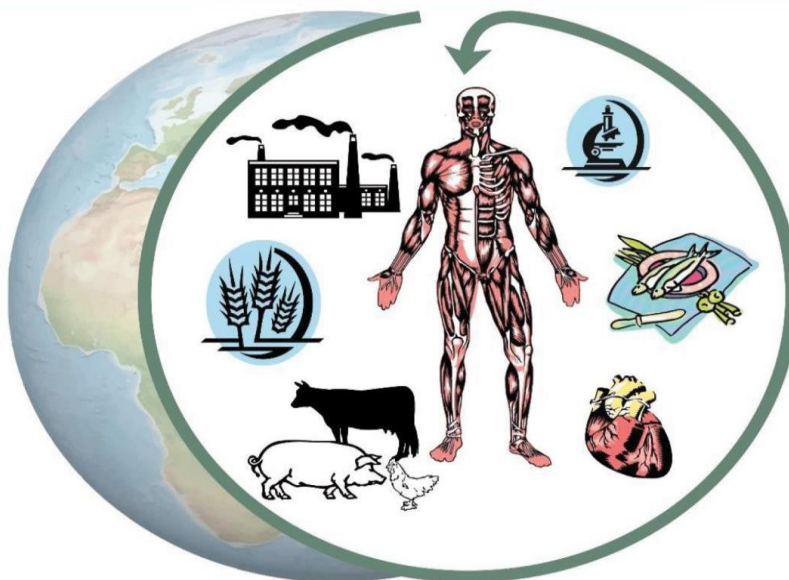
**Figure 1.** P-h diagram of the heat pump operating with one compressor, black cycle: non-insulated HP, green cycle: insulated HP.





**Figure 2.** P-h diagram of the HP operating with two compressors, black cycle: non-insulated HP, green cycle: insulated HP.

**Annex D.** Most important publications related to the thesis.



# 2023 RISK FACTORS OF FOOD CHAIN

XXIII. INTERNATIONAL CONFERENCE

---

BOOK OF ABSTRACTS

**MATE**  
HUNGARIAN UNIVERSITY OF  
AGRICULTURE AND LIFE SCIENCES

### **Editors**

Dr. Gábor GÉCZI, PhD  
Dr. Péter KORZENSZKY, PhD

### **Reviewers**

Dr. Péter SEMBERY, Professor emeritus,  
CSc Dr. Peter MASSÁNYI, Professor, DSc  
Dr. Norbert LUKÁČ, Professor, PhD  
Dr. Gábor Endre HALÁSZ, Associate professor, PhD

© Authors, 2022

© Editors, 2022

*This is an open access book under the terms and conditions of the Creative Commons attribution ([CC-BY-NC-ND](https://creativecommons.org/licenses/by-nc-nd/4.0/)) license 4.0.*



### **Published by**

Hungarian University of Agriculture and Life Sciences Szent István  
Campus H-2100 Gödöllő, Práter Károly u. 1.

Tel.: +36-28/522-000

<https://www.uni-mate.hu>

Under the supervision of Dr. András Béres, director general of Campus

Cover design: Norbert Szalai

ISBN 978-963-623-071-5 (pdf)

## ENERGY ANALYSIS OF REFRIGERATION CYCLES IN THE FOOD INDUSTRY

Hermanucz P.<sup>\*1</sup>, Herzallah L.<sup>1</sup>, Korzenszky P.<sup>2</sup>

<sup>1</sup> *Department of Building Engineering and Energetics, Institute of Technology*

<sup>2</sup> *Department of Farm and Food Machinery, Institute of Technology*

<sup>1,2</sup> *Hungarian University of Agriculture and Life Sciences, Gödöllő Hungary.*

<sup>\*</sup> [hermanucz.peter@uni-mate.hu](mailto:hermanucz.peter@uni-mate.hu)

Refrigeration is vital in the food industry because it preserves perishable products, inhibits bacterial growth, and maintains food quality and safety. This technology extends shelf life, reduces food waste, and ensures that consumers receive safe and fresh products, all of which are critical aspects of the food supply chain. To achieve these cooling processes, different types of cooling systems are used. Their operation not only has a significant impact on food quality, but also plays a significant role from an energy and environmental point of view. The energetics of cooling circuits are crucial because they directly impact energy efficiency and operating costs in refrigeration systems. Understanding and optimizing these energetics help reduce energy consumption, lower greenhouse gas emissions, and improve the sustainability of cooling processes, aligning with environmental and economic goals. In the food industry, various types of refrigerators are employed to cater to different needs. These include walk-in coolers and freezers for large-scale storage, reach-in refrigerators for easy access, blast freezers for rapid cooling, and display refrigerators to showcase products. The choice depends on specific requirements and product characteristics.

In this paper, we investigate the widely used compressor refrigeration system. Our aim is to investigate the energetics of a system with two compressors, so that the cooling power can be controlled simply by switching the compressors on and off, rather than using the modern technology of a frequency converter. The evaporating and condensing pressures of the system are the same as those used in standard refrigerators in the food industry. During the test, we measured the electrical power absorbed by the compressor and the thermal power absorbed by the evaporator, as well as the heat dissipation through the condenser. From the measurement results we determined the coefficient of performance (COP) of the system both when one compressor was running and when two compressors were running.

The results showed unexpected variations in cooling performance and hence coefficient of performance. It can be concluded that in certain operating conditions, the use of modern compressors with variable frequency drives would be significantly more favourable. Naturally, this will require further changes and improvements in the cooling system.

**Keywords:** refrigeration cycle, COP, energy efficiency